

First-Principles Phase Stability Calculations of Pseudobinary Alloys of $(\text{Al}, \text{Zn})_3\text{Ti}$ with $L1_2$, DO_{22} and DO_{23} Structures

Gautam Ghosh¹, Axel van de Walle¹ and Mark Asta²

¹*Department of Materials Science and Engineering,*

*Robert R. McCormick School of Engineering and Applied Science,
Northwestern University, 2220 Campus Drive, Evanston, IL 60208-3108, USA and*

²*Department of Chemical Engineering and Materials Science,*

*Center for Computational Science and Engineering,
University of California at Davis, Davis, CA 95616, USA*

The thermodynamic and mechanical stabilities of the $\text{Al}_3\text{Ti}-\text{Zn}_3\text{Ti}$ pseudobinary alloy system is investigated from first-principles through density-functional theory calculations within the generalized gradient approximation. Both supercells calculations and sublattice cluster expansion methods are used to demonstrate that the addition of Zn to the Al sublattice of Al_3Ti stabilizes the cubic $L1_2$ structure relative to the tetragonal DO_{22} and DO_{23} structures. This trend can be understood in terms of a simple rigid-band picture in which the addition of Zn modifies the effective number of valence electrons that populate bonding and anti-bonding states. The calculated zero-temperature elastic constants show that the binary end members are mechanically stable in all three ordered phases. These results point to a promising way to cost effectively achieve the stabilization of $L1_2$ precipitates in order to favor the formation of a microstructure associated with desirable mechanical properties.

I. INTRODUCTION

The trialuminide compounds with early transition metals (Sc, Ti, Zr, Hf, V, Nb, Ta) usually exhibit one or more of the three ordered structures based on the fcc lattice: cubic- $L1_2$, or tetragonal- DO_{22} and DO_{23} . The phase stability of cubic $L1_2$ -structured trialuminides is of fundamental importance for its use in at least two applications: (i) as potential high-temperature structural materials, and (ii) for the design of high-temperature, creep-resistant aluminum-based alloys containing coherent precipitates. Related to (ii), among binary alloy systems Al-Sc exhibits nanoscale precipitates of coherent $L1_2$ - Al_3Sc as an equilibrium phase in an (Al) matrix^{1,2}. However, the high cost of Sc limits its use in commercial alloys. Metastable Al_3Zr with the $L1_2$ structure, especially when alloyed with V, is used in commercial alloys as a grain refiner, and also to improve coarsening resistance and creep properties^{3,4}. However, with prolonged aging at high temperature $L1_2$ - Al_3Zr can be expected to transform to its equilibrium tetragonal structure (DO_{23}) with a resulting degradation of mechanical properties. Several Al-rare earth systems (RE=Er, Tm, Yb, Lu, Np) also exhibit $L1_2$ - Al_3RE compounds as equilibrium phases. However, the solubility of these RE elements in Al is extremely small, so that such Al-RE alloys are not readily amenable to heat treatment. Based on these considerations, in the design of Al alloys for high-temperature applications, it is of interest to explore ternary alloy compositions which can lead to the formation of a microstructure with nanoscale precipitates of a thermodynamically stable $L1_2$ phase. Due to the extremely slow diffusion rates of Ti in Al⁵, compositions based on the binary Al-Ti system are of particular interest for such applications.

The existence of ternary $L1_2$ phases based on Al_3Ti has been reported in several Al-Ti-X (X=V, Cr, Mn, Fe, Co, Ni, Cu, Zn, Nb, Mo, Rh, Pd, Ag, Pt, and Au) systems⁶. Among these systems, the available experimental ternary phase diagrams do not show an equilibrium tie-line between (Al) and the $L1_2$ phase due to intervening tie-lines involving Al-Ti and Al-X intermetallics, and some ternary compounds. Even though the phase equilibria of Al-Ti-Zn has not been fully investigated, this system offers the possibility of the existence of stable tie-lines between (Al) and a ternary $L1_2$ phase for the following reasons: (i) there are no Al-Zn intermetallic phases, (ii) the equilibrium $L1_2$ - TiZn_3 phase is known to dissolve a substantial amount of Al⁷, and (iii) ternary $L1_2$ phases are known to exist in the related Al-Zr-Zn and Al-Hf-Zn systems⁷. In the absence of experimental thermodynamic data for Zn-Ti and Al-Zn-Ti intermetallics, we seek to investigate the relative stability of the above-mentioned cubic and tetragonal ordered structures by first-principles methods which will ultimately facilitate the calculation of multicomponent phase diagrams within the Calphad formalism.

To investigate the relative stability of $L1_2$, DO_{22} and DO_{23} phases in Al-Ti-Zn alloys, we focus on the pseudobinary compositions $(\text{Al}_{1-x}\text{Zn}_x)_3\text{Ti}$. Along this line of compositions we are particularly interested in the composition dependence of the formation enthalpies as one moves from Al_3Ti , where the tetragonal structures are stable, to Zn_3Ti where the cubic $L1_2$ structure forms. In this investigation, we are thus required to compute the energies of intermetallic compounds with substitutional disorder on the Al/Zn sublattices. Within a first-principles framework we employ two complementary approaches for this purpose, namely (i) the use of supercell (SC) geometries, and (ii) the application

of a sublattice cluster-expansion (SCE) formalism¹⁶ which has been widely used to model anion and/or cation disorder in ceramic systems¹⁷. As described below, the SC approach involves calculations of the energy of structures where several crystallographically equivalent sites are created by repeating the unit cell along the principle lattice directions; the energies of compounds with site-substituted species are thus calculated at discrete compositions. The SCE method involves energy calculations for several ordered superstructures representing various configurations of Al and Zn atoms on the relevant sublattices, from which values for the effective cluster interaction (ECI) parameters in a cluster expansion for the energy are extracted; with such a cluster expansion the energy can be computed as a continuous function of composition. The complimentary nature of these two approaches will be illustrated below: while SC approach allows calculations for only a relatively few discrete calculations, it can be readily used to investigate the electronic-structure features underlying the relative stabilities of the competing compounds. Such electronic-structure information is not readily available from the SCE approach, although this method allows calculations of the energy as a continuous function of composition and effects of configuration short-range order (SRO) can be estimated through Monte-Carlo simulations based on the calculated ECIs.

The next section provides further details related to the application of the complementary first-principles SC and SCE methods in their application to the study of intermetallic phase stability in Al-Ti-Zn. We discuss in particular the details related to the implementation of the SCE approach, namely the algorithms for structure and cluster selection that underly its application within the automated ATAT software^{13,14}. The results of the calculations for formation energies and elastic constants are given in section III, and the effect of Zn additions in stabilizing the cubic $L1_2$ structure is discussed within a simple band-filling picture based on the calculated electronic densities of states of the competing intermetallic phases. The results and conclusions are summarized in the final section.

II. COMPUTATIONAL METHODOLOGY

The first-principles calculations presented here are based on electronic density-functional theory (DFT), and have been carried out using the *ab-initio* total-energy and molecular-dynamics program VASP (Vienna *ab-initio* simulation package)^{8,9}, employing ultrasoft pseudopotentials¹⁰, and an expansion of the electronic wavefunctions in plane waves with a kinetic-energy cutoff of 281 eV. All calculated results were derived employing the generalized gradient approximation (GGA) due to Perdew and Wang¹¹. The remaining computational details related to the density of k-point sampling and convergence criteria for structural optimizations are the same as those described in an earlier publication¹².

In this study, we are interested in the effect of Zn(or Al) on the relative stability of $(Al_{1-x}Zn_x)_3Ti$ phases in the $L1_2$, DO_{22} and DO_{23} structures. The conventional unit cells for each of these structures is illustrated in Fig. 1 where the Ti and Al/Zn sublattices are indicated by black and white circles, respectively. In the cubic $L1_2$ structure all of the Al/Zn sublattice sites are equivalent by symmetry. For the tetragonal DO_{22} structure there are two symmetry-distinct Al/Zn sublattice positions, namely the $2b$ site (located in the (001) planes containing both Ti and Al/Zn atoms) and $4d$ site (located in the (001) planes containing only Al/Zn atoms). The tetragonal DO_{23} structure contains three symmetry-distinct Al/Zn sublattice sites, namely the $4e$ sites located in the (001) planes containing both Ti and Al/Zn, and two distinct sites in the pure Al/Zn (001) planes, namely $4d$ and $4e$.

To model the compositional disorder on the Al/Zn sublattices for ternary alloy compositions, two first-principles approaches are employed. The first makes use of periodic supercell (SC) structures, where several crystallographically equivalent sites are created by repeating the original unit cell along the principle lattice directions and the energy of compounds with site-substituted species are derived at discrete compositions. In the second approach *ab-initio* energy calculations are combined with statistical methods within the framework of the sublattice cluster expansion (SCE) formalism¹⁶, allowing predictions of thermodynamic properties as a continuous function of composition and configurational order. The details associated with each of these approaches are described in the following two subsections.

A. Supercell calculations

In our application of the SC approach we have calculated the total energies of ternary alloys using supercells of $2 \times 2 \times 2$ primitive cells for $L1_2$, and $2 \times 2 \times 1$ for DO_{22} and DO_{23} structures. For the latter two structures, these supercells have dimensions of $2 \times 2 \times 2$ fcc unit cells for DO_{22} and $2 \times 2 \times 4$ fcc unit cells for DO_{23} (c.f. Fig. 1).

For the $L1_2$ structure the supercell contains 32 total sites, with 8 Ti atoms and the remaining 24 sites occupied by Al or Zn. Five compositions were considered for this structure, namely: (i) Al_3Ti , (ii) $(Al_{0.667}Zn_{0.333})_3Ti$, (iii) $(Al_{0.5}Zn_{0.5})_3Ti$, (iv) $(Al_{0.333}Zn_{0.667})_3Ti$, and (v) Zn_3Ti . For the ternary compositions, the atoms on the Al/Zn sublattice were arranged in an ordered manner with the minority species (for compositions (ii) and (iii)) having both like and unlike nearest neighbors. The DO_{22} and DO_{23} supercells contained 32 and 64 sites, respectively. For both

phases we considered four compositions: (i) Al₃Ti, (ii) (Al_{0.667}Zn_{0.333})₃Ti, (iii) (Al_{0.333}Zn_{0.667})₃Ti, and (iv) Zn₃Ti. For the *DO*₂₂ supercell compositions (ii) and (iii) were constructed by placing the minority and majority species in the 2*b*-type and 4*d* sites, respectively. In the case of the *DO*₂₃ structure, total energies for compositions (ii) and (iii) were calculated by substituting Zn (or Al) in all three unique sites, 4*c*, 4*d* and 4*e*, of Al₃Ti (or Zn₃Ti); the configuration that gave the minimum energy was used for the analysis of relative phase stability. For each structure the energies were computed by first principles performing full structural optimizations with respect to volume and all (cell internal and cell external) crystallographic degrees of freedom.

B. Cluster expansion and Monte Carlo simulations

Within the cluster expansion (CE) formalism, the dependence of the total energy E (per unit cell) of a binary alloy on the atomic configuration σ on a given lattice is represented in the form¹⁸

$$E(\sigma) = \sum_{\alpha} m_{\alpha} J_{\alpha} \langle \sigma_{\alpha'} \rangle \quad (1)$$

where the σ_i are so-called occupation variables taking the value -1 or $+1$, depending on which type of atom occupies site i and where $\sigma_{\alpha} \equiv \prod_{i \in \alpha} \sigma_i$. The sum extends over all clusters α that are symmetrically distinct while the average $\langle \rangle$ is taken over all clusters α' that are equivalent by symmetry to α . The m_{α} are multiplicity coefficients equal to the number of clusters (per unit cell) equivalent to α by symmetry. The effective cluster interactions (ECI) J_{α} are interactions coefficients to be determined by a fit to formation energies obtained from first-principles.

Although atomic displacements do not explicitly appear in (1), their effect is implicitly included in the coefficients J_{α} . That is, $E(\sigma)$ is actually the energy of the alloy after internal relaxations of the atomic positions and of cell parameters have taken place. In principle, the cluster expansion provides an exact representation of the configurational dependence of the energy if the sum extends over every possible clusters. In practice, the expansion is truncated to a finite number of terms that is sufficient to provide the desired accuracy. If one had knowledge of the energy of every possible configuration σ , the ECI could be exactly calculated from

$$J_{\alpha} = 2^{-\#\alpha} (\langle E(\sigma) | \sigma_{\alpha} = 1 \rangle - \langle E(\sigma) | \sigma_{\alpha} = -1 \rangle) \quad (2)$$

where $\#\alpha$ is the number of sites in α and the averages $\langle \rangle$ are taken over all configurations σ such that σ_{α} for the selected cluster α takes on a specific value. For some intuition, consider the special case of a Hamiltonian consisting purely of nearest neighbor interactions. Equation (2) when α is a nearest neighbor pair would then simply reduce to half the difference between the average bond energy between like and unlike atoms (i.e. $(E_{AA} + E_{BB})/2 - E_{AB}/2$, where E_{ts} represent bond energies between atoms of type t and s). In practice, only a finite number of structural formation energies are calculated from first-principles and the ECI are not determined by Equation (2) but rather by a fit of Equation (1), truncated to a finite number of terms, to the known energies.

A sublattice cluster expansion (SCE) takes the same form as Equation (1) and, formally, each ECI is also exactly given by Equation (2). The efficacy of the sublattice cluster expansion method in understanding phase stability and phase equilibria has been demonstrated in multicomponent oxide systems^{16,17}. In this study, the unit cells of *L*1₂, *DO*₂₂ and *DO*₂₃ structures are considered, allowing occupation of Zn in the Al-sublattice(s) (or Al in Zn-sublattice(s)), while, in the other sublattice, Ti acts as a spectator specie. The spectator atoms do not explicitly enter the expression of the cluster expansion because their configuration on their respective sublattice does not change. However, their presence modifies the construction of the cluster expansion in two important ways. First, the energy $E(\sigma)$ in Equations (1) and (2) includes the contribution of the spectator species so that the ECI coupling two sites also includes the indirect interaction between these sites mediated through the spectator specie. For instance, if a “larger” atom on site i pushes the spectator atom away in such a way that an atom on site j has “less room”, the ECI $J_{\{i,j\}}$ coupling sites i and j will account for that energy cost, even though the spectator specie resides neither on site i nor j . The spectator atoms can also mediate interactions of a chemical nature (e.g. electronegativity differences on site i can affect the effective valence of a spectator specie, which, in turn, modifies the relative energy cost of placing different species on site j). The second important effect of the spectator species is that they lower the symmetry of the sublattice of interest, so that the ECI associated with two clusters that have apparently identical geometries may still differ due to differing environments. For instance, in Figure 3(a) and Table IV, clusters 2 and 3 for the *L*1₂ lattice have identical lengths but are considered different because cluster 2 goes through a dumbbell on spectator atoms while cluster 3 does not. Formally, cluster equivalence is determined according to the joint space group of the two sublattices.

The cluster expansion for each of the three lattices considered (see Fig. 1) were constructed using the Alloy Theoretic Automated Toolkit (ATAT) package^{13,14}. ATAT proceeds by gradually increasing the number of clusters included in the cluster expansion and the number of structures used to fit the ECI, until the user is satisfied with the accuracy

of the cluster expansion. As an example, Fig 2 plots the formation energies of the structures used for the cluster expansion of $L1_2$ pseudobinary alloy. In this representation, the ground states in this system can be determined by identifying the points touching the convex hull. For a given set of structural energies, the optimal set of clusters is determined by minimizing the cross-validation (CV) score, defined as $(\sum_s (E_s - \bar{E}_s)^2)^{(1/2)}$, where E_s is the energy of structure s while \bar{E}_s the energy predicted from the cluster expansion using all structures except structure s . The database of structures used in the fit of the cluster expansion is gradually enlarged by adding structures that differ as much as possible from the structures already considered in terms of the correlations $\langle \sigma_\alpha \rangle$.

III. RESULTS AND DISCUSSION

In this section the results of first-principles calculations are presented related to the relative stability of the competing $L1_2$, DO_{22} and DO_{23} structures for the pseudobinary compositions $(Al_{1-x}Zn_x)_3Ti$. The first two subsections concern the structural, energetic and elastic properties of the binary end-member compositions. The third subsection presents the composition dependencies of the formation energies for each of the three structures calculated by the supercell and sublattice-cluster-expansion methods described above. These results show that the $L1_2$ structure is energetically stable over a wide range of Zn compositions. In the final subsection the origin of the stabilizing effect of Zn is discussed in terms of a band-filling picture based on the calculated electronic densities of states.

A. Structural Properties and Phase stability of Al_3Ti and Zn_3Ti

The total energies of Al_3Ti and Zn_3Ti having $L1_2$, DO_{22} , DO_{23} structures were each calculated as a function of volume, with all of the structural degrees of freedom being reoptimized at each volume. The resulting total energies were then fit to an equation of state (EOS)¹⁹ defining the relationship between pressure (P) and volume (V) at zero temperature. From the EOS, the equilibrium energy and atomic volume (V_o), as well as the bulk modulus (B_0) and its pressure derivative (B'_0) were derived for all three structures. The results are given in Table I, along with the calculated zero-temperature formation energies (ΔE_f), defined as the difference in energy between the compound and the concentration-weighted average of the energies of the constituent atomic species in the reference crystal structures given in the Table caption.

Considering specifically the formation-energy values, we note that, consistent with the results of earlier calculations (discussed in detail elsewhere¹²), DO_{23} is calculated to be the ground state (i.e., the lowest-energy structure at zero temperature) for the Al_3Ti composition. The crystal chemistry of Zn-Ti intermetallics has been summarized by Vassilev *et al.*²⁰, and $L1_2$ - Zn_3Ti is known to be stable at low temperature, while the tetragonal structures DO_{22} and DO_{23} have not been observed. Consistent with these observations, we find that $L1_2$ - Zn_3Ti is the ground state structure whereas DO_{22} and DO_{23} have significantly higher energies²¹. It is noteworthy that unlike the Al_3Ti system, DO_{22} - Zn_3Ti is far less stable compared to DO_{23} - Zn_3Ti .

B. Mechanical stability of Al_3Ti and Zn_3Ti

In considering the relative thermodynamic stability of competing stable and metastable phases, it is important to consider whether the higher energy structures are truly metastable or whether they are mechanically or dynamically unstable in their bulk form. This issue of mechanical stability can be assessed by calculating the single-crystal elastic constants. Generally, the single-crystal elastic constants can be obtained by *ab-initio* electronic-structure methods by calculating the total energy as a function of appropriate lattice deformations. Depending on the crystal system and the type of imposed lattice deformation, the curvature of the total energy versus strain curves define either a particular elastic constant or a combination of elastic constants. In this study, we have calculated single crystal elastic constants of six binary intermetallics (Al_3Ti and Zn_3Ti with $L1_2$, DO_{22} and DO_{23} structures) defining the end members of the pseudo-binary section Al_3Ti - Zn_3Ti .

The internal energy ($E(V, \{e_i\})$) of a crystal under an infinitesimal strain e_i , referenced to the energy of the equilibrium geometry, can be written as

$$E(V, \{e_i\}) = E(V_o, 0) + \frac{V_o}{2} \sum_{ij} C_{ij} e_i e_j + \dots \quad (3)$$

where V_o is the volume of the unstrained crystal with $E(V_o, 0)$ being the corresponding energy, C_{ij} s are the single crystal elastic constants, and the members of strain tensor $\varepsilon\{e_i, e_j, \dots\}$ are given in Voigt notation.

TABLE I: Equilibrium cohesive properties at 0 K, as defined by the equation of state (EOS), of Al₃Ti and Zn₃Ti having one of three possible structures. The units of lattice constants, V_0 , B_0 and ΔE_f (with respect to fcc-Al, hcp-Ti and hcp-Zn) are nm, 10^{-3} nm³/atom, 10¹⁰ N/m² and kJ/mol, respectively. The equilibrium cell-internal degrees of freedom (Wyckoff positions) in the DO_{23} structure are also provided.

Phase	Structure	EOS parameters	ΔE_f	Lattice constants	Wyckoff positions (x, y, z) (with degree(s) of freedom)
		V_0	B_0	B'_0	
Al ₃ Ti	$L1_2$ (<i>Pm</i> $\bar{3}m$)	15.737	10.36	4.12	-36.583 $a=0.39779$
	DO_{22} (<i>I4/mmm</i>)	15.929	10.30	4.15	-38.895 $a=0.38399$ $c=0.86399$
	DO_{23} (<i>I4/mmm</i>)	15.819	10.31	4.08	-39.656 $a=0.38962$ $c=1.66713$ Al1(4c): 0.0, $\frac{1}{2}$, 0.0 Al2(4d): 0.0, $\frac{1}{2}$, $\frac{1}{4}$ Al3(4e): 0.0, 0.0, 0.37519 Ti(4e): 0.0, 0.0, 0.11875
Zn ₃ Ti	$L1_2$ (<i>Pm</i> $\bar{3}m$)	15.143	9.92	5.05	-19.177 $a=0.39273$
	DO_{22} (<i>I4/mmm</i>)	14.967	10.05	5.18	-9.103 $a=0.43355$ $c=0.61323$
	DO_{23} (<i>I4/mmm</i>)	15.131	9.71	5.67	-14.973 $a=0.40363$ $c=1.48459$ Ti(4e): 0.0, 0.0, 0.12540 Zn1(4c): 0.0, $\frac{1}{2}$, 0.0 Zn2(4d): 0.0, $\frac{1}{2}$, $\frac{1}{4}$ Zn3(4e): 0.0, 0.0, 0.36827

For the $L1_2$ structure with cubic lattice symmetry, there are three single-crystal elastic constants, C_{11} , C_{12} and C_{44} . For the DO_{22} and DO_{23} phases with tetragonal lattice symmetry, there are six single-crystal elastic constants, C_{11} , C_{12} , C_{13} , C_{33} , C_{44} and C_{66} . For both cubic and tetragonal structures, Mehl *et al.*²² have summarized the appropriate lattice deformations needed to derive the C_{ij} s. Accordingly, we have calculated total energies by imposing appropriate strains up to $\pm 3\%$ at 0.5% intervals. The total energies versus strain were then fit with the functional forms provided by Mehl *et al.*²² to extract the elastic moduli.

The calculated C_{ij} s of Al₃Ti and Zn₃Ti phases having $L1_2$, DO_{22} and DO_{23} structures are listed in Tables II and III, respectively. For DO_{22} -Al₃Ti, our results are compared with available experimental data²⁵, as well as previous *ab initio* values for $L1_2$ and DO_{22} structures calculated by DFT within the local-density approximation (LDA), using the full-potential linearized augmented plane-wave method^{23,24}. A comparison of experimental data²⁵ with our calculated values for the DO_{22} structure shows very good agreement for the values of C_{13} , C_{33} , C_{44} and C_{66} in Al₃Ti. In a previous calculation^{23,24}, these values were computed to be consistently higher than the present values, which is likely due to the use of the LDA approximation which is known to consistently lead to predictions of smaller equilibrium volumes and larger elastic moduli relative to the GGA used here. In both the present (GGA) and previous (LDA) calculations the value of C_{11} shows a reasonable agreement with experimental data. However, both the present and previous calculations predict C_{12} in Al₃Ti to be significantly higher than the measured value.

TABLE II: Calculated zero-temperature single-crystal elastic constants (in $\times 10^{10}$ N/m²) of Al₃Ti in the $L1_2$, DO_{22} , and DO_{23} structures. Our calculated C_{ij} s are compared with previous ab initio and experimental data.

Al ₃ Ti (This study)			Al ₃ Ti (Previous results)		
$L1_2$	DO_{22}	DO_{23}	$L1_2$, ab initio ^a	DO_{22} , ab initio ^b	DO_{22} , expt. ^c
$C_{11}=18.39$	$C_{11}=19.23$	$C_{11}=20.79$	$C_{11}=17.70$	$C_{11}=20.20$	$C_{11}=21.77$
$C_{12}=6.26$	$C_{12}=8.28$	$C_{12}=6.35$	$C_{12}=7.70$	$C_{12}=8.80$	$C_{12}=5.77$
$C_{44}=7.35$	$C_{13}=4.49$	$C_{13}=4.72$	$C_{44}=8.50$	$C_{13}=6.00$	$C_{13}=4.55$
	$C_{33}=21.25$	$C_{33}=20.56$		$C_{33}=24.30$	$C_{33}=21.75$
	$C_{44}=9.30$	$C_{44}=8.33$		$C_{44}=10.0$	$C_{44}=9.20$
	$C_{66}=12.84$	$C_{66}=10.16$		$C_{66}=14.50$	$C_{66}=11.65$

^aFPLAPW-LDA method²³

^bFPLAPW-LDA method^{23,24}

^cref.²⁵

The requirements of mechanical stability in a cubic crystal are²⁶: $C_{11} > 0$, $C_{12} > 0$, $(C_{11} - C_{12}) > 0$, $C_{44} > 0$. Similarly, the requirements of mechanical stability in a tetragonal crystal are²⁶: $C_{11} > 0$, $C_{12} > 0$, $C_{13} > 0$, $C_{33} > 0$, $C_{44} > 0$, $C_{66} > 0$, $(C_{11} - C_{12}) > 0$, $(C_{11} + C_{33} - 2C_{13}) > 0$, and $(2C_{11} + C_{33} + 2C_{12} - 4C_{13}) > 0$. In Tables II and III, it is important to note that even though $L1_2$ -Al₃Ti, DO_{22} -Al₃Ti, DO_{22} -Zn₃Ti and DO_{23} -Zn₃Ti are not the lowest-energy

TABLE III: Calculated zero-temperature single-crystal elastic constants (in $\times 10^{10}$ N/m²) of Zn₃Ti in the *L1₂*, *DO₂₂*, and *DO₂₃* structures.

Zn ₃ Ti (this study)		
<i>L1₂</i>	<i>DO₂₂</i>	<i>DO₂₃</i>
$C_{11}=12.25$	$C_{11}=16.66$	$C_{11}=16.68$
$C_{12}=8.79$	$C_{12}=4.36$	$C_{12}=5.38$
$C_{44}=7.27$	$C_{13}=8.69$	$C_{13}=7.71$
	$C_{33}=12.36$	$C_{33}=12.69$
	$C_{44}=5.65$	$C_{44}=7.32$
	$C_{66}=1.73$	$C_{66}=5.46$

structures, they satisfy the criteria of mechanically stability. These results imply that it is unlikely that any of these structures will be mechanically unstable at intermediate compositions along the pseudo-binary section.

C. Effective cluster interaction (ECI) parameters

The ECIs obtained from cluster expansions are given in Table IV. The databases of structures used for the cluster expansion fit are reported in Tables V, VI and VII in the appendix. The clusters selected are schematically shown in Fig. 3. The fitted ECIs are plotted in Fig. 4 as a function of normalized interaction range. In all cases the alloy energetics is dominated by (pseudo)pair interactions, except that there is one (pseudo)three-body interaction in *DO₂₂*. A major difference between the structures is that in *L1₂* all ECIs are positive while in *DO₂₂* and *DO₂₃* the ECIs are both positive and negative. Understanding the origin of this difference is complicated by the differing crystal symmetry, number of non-equivalent Al (or Zn) sites, different arrangement of spectator specie (Ti), and differences in bond lengths associated with tetragonal distortions in these different structures. It is to be noted that Fig. 4 also reports the CV score for each cluster expansion, which provide estimates of the predictive power of each cluster expansion and can be used to derive error bars on the predicted enthalpies.

In this work, we employ the cluster expansions constructed above to predict the enthalpy of formation of solid solutions in two ways. First, in the limit of a fully disordered alloy (i.e. in the Bragg-Williams approximation), the enthalpy of the alloy at composition $0 < x < 1$ is given by

$$H(x) = \sum_{\alpha} m_{\alpha} J_{\alpha} (2x - 1)^{\# \alpha} \quad (4)$$

where we have used the fact that $\langle \sigma_{\alpha} \rangle = \prod_{i \in \alpha} \langle \sigma_i \rangle = (2x - 1)^{\# \alpha}$ if the occupation of the sites is perfectly random. A more accurate way to calculate the enthalpy of the alloy is to employ lattice-gas Monte Carlo simulations using the cluster expansion to calculate the alloy energy (e.g.¹⁵). The microscopic states can then be sampled with a probability equal to the Boltzman factor, thus allowing for the possible presence of short-range order.

D. Phase stability along Al₃Ti-Zn₃Ti

Figure 5 shows a comparison of the formation energies of the *L1₂* and *DO₂₂* structures, as a function of Zn concentration along the psedubinary section (Al_{1-x}Zn_x)₃Ti, calculated by cluster expansion (or random approximation) and Monte-Carlo simulation to include the effect of short-range ordering. In Fig. 5(a) and Fig. 5(b), the solid line corresponds to calculated formation energy due to random mixing of Al and Zn in 3c site of *L1₂* structure and in 2b and 4d sites of *DO₂₂* structures, while triangles and + symbols represent the calculated formation energy accounting for short range ordering in Monte-Carlo simulations at 2000 and 1000 K, respectively. As the temperature is lowered, strong ordering or clustering tendencies would be manifested in a pronounced temperature dependence of the calculated formation energies, which is seen to be absent in the Monte-Carlo results.

Figure 6 represents the central result of the current study. It plots the calculated formation energies of the *L1₂*-, *DO₂₂*- and *DO₂₃* structures as a function of Zn concentration along the psedubinary section (Al_{1-x}Zn_x)₃Ti. As discussed above, the *L1₂* structure has the lowest energy for the composition Zn₃Ti, while it is significantly higher in energy than the tetragonal *DO₂₂* and *DO₂₃* structures for Al₃Ti. For the ternary compositions, the filled circles and solid lines represent the results of the supercell and sublattice-cluster-expansion calculations, respectively, which are seen to be in good overall agreement. The most striking feature of the results concerns the effect of Zn additions starting from the Al₃Ti composition. While such additions increase the energy of both tetragonal structures, Zn is

TABLE IV: Effective cluster interaction parameters (ECIs) in $L1_2-(Al_{1-x}Zn_x)_3Ti$, $DO_{22}-(Al_{1-x}Zn_x)_3Ti$, and $DO_{23}-(Al_{1-x}Zn_x)_3Ti$. The empty, point, pair and three-body clusters are labeled as $E(0,1)$, $E(1,1....n)$, $E(2,1....n)$, and $E(3,1....n)$, respectively. It may be noted that there are two and three point clusters in DO_{22} and DO_{23} phases, respectively, due to two ($2b$, $4d$) and three ($4c$, $4d$, $4e$) Wyckoff positions for Al (or Zn) in the corresponding structure. Unlike ECIs in a binary alloy system, the pair and three-body interaction parameters in a pseudo-binary system should be considered as pseudo-pair and pseudo-three-body interaction parameters due to the interactions with the spectator specie. Coordinates are in fraction of lattice vectors (the z coordinates for the DO_{23} lattice are rounded to the nearest $1/8$, for clarity). Cluster size is defined as the length of the longest pair contained in the cluster (calculated using the lattice parameters of Al_3Ti in the corresponding structure).

Phase	Cluster symbol	Cluster coordinates	Cluster size (nm)	Multiplicity	ECI (meV/cluster)
$L1_2-(Al_{1-x}Zn_x)_3Ti$	$E(0,1)$				-261.193
	$E(1,1)$	(0.0,0.5,0.5)		3	5.531
	$E(2,1)$	(0.0,0.5,0.5) (0.5,0.0,0.5)	0.28072	12	8.913
	$E(2,2)$	(0.5,0.5,0.0) (-0.5,0.5,0.0)	0.39700	6	4.303
	$E(2,3)$	(0.5,0.5,0.0) (0.5,0.5,1.0)	0.39700	3	1.403
	$E(2,4)$	(1.0,0.5,0.5) (0.5,-0.5,0.0)	0.48622	24	2.612
	$E(2,5)$	(0.5,0.5,1.0) (-0.5,0.5,0.0)	0.56144	12	0.986
	$E(2,6)$	(0.5,0.0,0.5) (-0.5,0.0,-0.5)	0.56144	6	3.247
	$E(2,7)$	(1.0,0.5,0.5) (-0.5,0.5,0.0)	0.62771	24	0.700
	$E(2,8)$	(0.5,0.0,0.5) (-0.5,1.0,-0.5)	0.68762	12	0.161
	$E(2,9)$	(1.0,0.5,0.5) (-0.5,-0.5,0.0)	0.74272	48	0.503
$DO_{22}-(Al_{1-x}Zn_x)_3Ti$	$E(0,1)$				160.723
	$E(1,1)$	(0.0,0.0,0.5)		4	62.684
	$E(1,2)$	(0.0,0.5,0.25)		2	-9.547
	$E(2,1)$	(0.0,0.5,0.25) (0.5,0.0,0.25)	0.27152	8	-9.955
	$E(2,2)$	(0.0,0.5,0.25) (0.5,0.5,0.0)	0.28899	16	-4.177
	$E(2,3)$	(0.0,0.5,0.25) (1.0,0.5,0.25)	0.38399	8	-0.581
	$E(2,4)$	(0.0,0.0,0.5) (0.0,1.0,0.5)	0.38399	4	5.293
	$E(2,5)$	(0.5,0.0,0.25) (0.5,0.0,-0.25)	0.43199	4	-2.299
	$E(2,6)$	(1.0,0.5,0.25) (0.5,-0.5,0.0)	0.48059	32	0.000
	$E(2,7)$	(0.5,0.0,0.25) (0.0,0.5,-0.25)	0.51024	16	0.333
	$E(2,8)$	(0.5,0.5,0.0) (0.0,0.0,0.5)	0.51024	8	-0.364
	$E(2,9)$	(0.0,0.5,0.25) (1.0,-0.5,0.25)	0.54304	8	0.000
	$E(2,10)$	(0.0,1.0,0.5) (1.0,0.0,0.5)	0.54304	4	3.891
	$E(3,1)$	(0.5,0.5,0.0) (0.5,0.0,0.25) (0.0,0.5,0.25)	0.28899	16	-2.886
$DO_{23}-(Al_{1-x}Zn_x)_3Ti$	$E(0,1)$				-234.551
	$E(1,1)$	(0.0,0.5,0.0)		4	-15.924
	$E(1,2)$	(0.0,0.5,0.25)		4	1.755
	$E(1,3)$	(0.0,0.0,0.375)		4	15.433
	$E(2,1)$	(0.0,0.5,0.25) (0.5,0.0,0.25)	0.27550	8	-7.405
	$E(2,2)$	(0.0,0.5,0.0) (0.5,0.0,0.0)	0.27550	8	9.757
	$E(2,3)$	(0.0,0.5,0.5) (0.0,0.0,0.375)	0.28506	16	8.459
	$E(2,4)$	(0.0,0.5,0.25) (0.5,0.5,0.125)	0.28552	16	-1.111
	$E(2,5)$	(0.5,0.5,0.125) (-0.5,0.5,0.125)	0.38962	8	0.000
	$E(2,6)$	(0.5,0.0,0.0) (-0.5,0.0,0.0)	0.38962	4	0.000
	$E(2,7)$	(0.0,0.5,0.25) (0.0,-0.5,0.25)	0.38962	8	0.000
	$E(2,8)$	(0.0,0.5,0.5) (0.0,-0.5,0.5)	0.38962	4	0.000
	$E(2,9)$	(0.0,0.0,0.625) (0.0,0.0,0.375)	0.41621	2	-1.443
	$E(2,10)$	(0.5,0.0,0.0) (0.5,0.0,0.25)	0.41685	8	7.158

seen to lower the formation energy for the cubic $L1_2$ phase. For Zn site fractions greater than approximately 12 %, the $L1_2$ phase is seen to have the lowest energy.

The pronounced effect of Zn on the stability of the $L1_2$ phase is related to the relatively strong and negative mixing energy in this phase. The mixing energy, which is defined as the difference in energy between a ternary $(Al_{1-x}Zn_x)_3Ti$ alloy and the concentration-weighted average of the energies of Al_3Ti and Zn_3Ti with the same crystal structure, is plotted in Fig. 2 for the $L1_2$ structure. In Fig. 6 the mixing energy represents the difference between the formation energies plotted by the solid lines, and the dashed lines representing ideal behavior. The mixing energy for cubic

$L1_2$ is seen to be negative and relatively large in magnitude compared to the results for the tetragonal DO_{22} and DO_{23} compounds. Some insight into the qualitatively different mixing energies for the cubic versus the tetragonal structures can be obtained by considering the magnitudes of the effective cluster interactions plotted in Fig. 4. For each of the three structures the energetics of mixing on the Al/Zn sublattice are predicted to be dominated by pairwise interactions. For the $L1_2$ structure these ECIs are seen to be positive, favoring mixing, for all of the pairs selected by the ATAT algorithms in the generation of the sublattice cluster expansion. For the tetragonal DO_{22} and DO_{23} phases, by contrast, the pair interactions are seen to oscillate in sign, with unlike bonds favored energetically for some of the pairs and like bonds favored for others. The result of such frustrated ordering behavior is a near cancellation of bonding and clustering terms in the energy, leading to nearly ideal mixing behavior for Al and Zn in these tetragonal structures. Further analysis related to the stabilizing effect of Zn on the $L1_2$ structure relative to DO_{23} and DO_{22} will be presented in the next subsection in terms of calculated electronic densities of states.

It is interesting to consider further the relatively good agreement displayed between cluster-expansion and supercell results in Fig. 6. Specifically, the SC method makes use of particular ordered configurations to model the composition dependence of the formation energy, while the SCE results plotted in Fig. 6 correspond to random configurations. Good agreement between the two results implies that the difference in energy between ordered and random configurations are relatively small in this system. This interpretation is supported by the results of SCE-based Monte-Carlo simulations performed as a function of temperature for the $L1_2$ and DO_{22} phases plotted in Fig. 5. In systems where ordering tendencies are more pronounced, the good level of agreement between SC and SCE methods found here may not be generally expected, and the SCE approach, while computationally more demanding, is generally preferred as it provides a framework for incorporating configurational effects in calculations of alloy formation energies.

E. Electronic density of states along $\text{Al}_3\text{Ti-Zn}_3\text{Ti}$

Further insight into the origin of the stabilizing effect of Zn upon the stability of the cubic $L1_2$ relative to the tetragonal DO_{22} and DO_{23} structures can be gained by considering the calculated electronic densities of states shown in Fig. 7. We start with the results for Al_3Ti shown in panel (a). For each structure the DOS are characterized by a pronounced dip near the Fermi level. This so-called pseudo-gap feature²⁷ has been extensively discussed in the literature as reflecting a separation between bonding and antibonding states associated with hybridization between the Al p and Ti d electrons. At the Al_3Ti composition the $L1_2$ structure has its Fermi level lying to the right (i.e., at higher energies) relative to the pseudo-gap minimum, while for the tetragonal structures the Fermi levels are within or just to the left (lower energies) of the pseudo-gap. These results suggest that the stability of the tetragonal structures relative to cubic $L1_2$ can be interpreted as a reflection of the increased occupation of antibonding states in the latter²⁷. Based on this interpretation, a rigid-band model would predict that substitution of Al by Zn should increase the stability of $L1_2$ relative to DO_{22} and DO_{23} phases since Zn has one less valence electron than Al, and alloying with this element should have the effect of moving the Fermi level to lower energies relative to the pseudo-gap minima.

The results in panel (b), obtained for supercells with composition $(\text{Al}_{0.667}\text{Zn}_{0.333})_3\text{Ti}$, are in qualitative agreement with this band-filling picture. The Fermi level for the $L1_2$ structure is seen to lie within the pseudo-gap minimum, corresponding to near optimal filling of the bonding states. By contrast the Fermi level has moved to the left, leading to lower occupations of the bonding states, for the tetragonal structures. The stabilization of the $L1_2$ structure and destabilization of the tetragonal structures induced by substituting Zn for Al are thus entirely consistent with a band-filling picture where the reduction of electron per atom ratio leads to optimum filling of bonding states in the cubic phase (increasing cohesion) and decreased occupation of these states in DO_{22} and DO_{23} (leading to decreased cohesion).

The results in panel (c), for the composition $(\text{Al}_{0.333}\text{Zn}_{0.667})_3\text{Ti}$ where Fig. 6 shows a maximum energy difference between $L1_2$ and the higher-energy tetragonal structures, remain qualitatively consistent with the band-filling picture described in the previous two paragraphs. The results in panel (d), however, show qualitative differences in the shapes of the DOS, particularly for the tetragonal structures, indicating the limitations of the rigid-band model applied over the entire composition range.

IV. CONCLUSION

The thermodynamic and mechanical stabilities of the $L1_2$, DO_{22} and DO_{23} structures along the pseudo-binary section $\text{Al}_3\text{Ti-Zn}_3\text{Ti}$ were investigated via first-principles methods.

The relative thermodynamic stability of the structures considered was investigated by both supercell and cluster expansion methods. Due to the relatively small energy differences between ordered and disordered states (on the Al/Zn

sublattice) in this system, the supercell and cluster expansion methods give very similar results. Another consequence of this fact is that the Bragg-Williams approximation is reliable in this system and agrees with more accurate Monte Carlo simulations that could have accounted for the presence of short-range order if it had been present in this system.

While the thermodynamically stable structure of Al_3Ti is DO_{23} , the substitution of Zn on the Al sublattice of Al_3Ti is found to stabilize the $L1_2$ structure relative to the DO_{22} and DO_{23} structures. These trends can be intuitively understood in terms of a simple rigid-band picture in which the addition of Zn reduces the effective number of valence electrons. The fermi level in DO_{22} and DO_{23} Al_3Ti lies in a pseudo-gap, which is indicative of increased stability. In contrast, the fermi level lies in the antibonding states in the $L1_2$ structure. The addition of Zn lowers the fermi level, moving it towards optimal filling of the bonding states the $L1_2$ structure but away from optimal filling in the case of the DO_{22} and DO_{23} structures, thus stabilizing the $L1_2$ structure relative to the other two.

Our result thus indicate that Zn substitution in Al_3Ti alloys represents a promising way to achieve the stabilization of $L1_2$ precipitates in order to favor the formation of a microstructure associated with desirable mechanical properties.

The calculated zero-temperature elastic constants show that the binary end members are mechanically stable in all three ordered structures, suggesting that the compounds and solid solutions considered in this study are experimentally accessible.

V. APPENDIX

TABLE V: Description of the structures used in the cluster-expansion fit to calculate the formation energy of $L1_2(\text{Al}_{1-x}\text{Zn}_x)_3\text{Ti}$. Here, the formation energies (ΔE_f) are relative to $L1_2\text{-Al}_3\text{Ti}$ and $L1_2\text{-Zn}_3\text{Ti}$.

Structure ID (Composition)	Space Group (#)	Wyckoff position Site	(x, y, z)	$a/b/c$ (nm)	$\alpha/\beta/\gamma$	ΔE_f (eV/atom)
0 (Al_3Ti)	$Pm\bar{3}m$ (221)	Al: 3c	(0.50000, 0.50000, 0.00000)	0.39787		0.0
		Ti: 1a	(0.00000, 0.00000, 0.00000)			
2 ($(\text{Al}_{0.667}\text{Zn}_{0.333})_3\text{Ti}$)	$P4/mmm$ (123)	Al: 2e	(0.50000, 0.00000, 0.50000)	0.39765		-0.091933
		Zn: 1c	(0.50000, 0.50000, 0.00000)			
		Ti: 1a	(0.00000, 0.00000, 0.00000)	0.38887		
3 ($(\text{Al}_{0.333}\text{Zn}_{0.667})_3\text{Ti}$)	$P4/mmm$ (123)	Al: 1c	(0.50000, 0.50000, 0.00000)	0.39061		-0.084757
		Zn: 2e	(0.50000, 0.00000, 0.50000)			
		Ti: 1a	(0.00000, 0.00000, 0.00000)	0.39787		
4 ($(\text{Al}_{0.833}\text{Zn}_{0.167})_3\text{Ti}$)	$P4/mmm$ (123)	Al1: 1c	(0.50000, 0.50000, 0.00000)	0.39793		-0.050068
		Al2: 4i	(0.00000, 0.50000, 0.74604)			
		Zn: 1d	(0.50000, 0.50000, 0.50000)	0.78585		
		Ti: 1a	(0.00000, 0.00000, 0.00000)			
		Ti: 1b	(0.00000, 0.00000, 0.50000)			
5 ($(\text{Al}_{0.833}\text{Zn}_{0.167})_3\text{Ti}$)	$Pmmm$ (47)	Al1: 1c	(0.00000, 0.00000, 0.50000)	0.79461		-0.054040
		Al2: 1d	(0.50000, 0.00000, 0.50000)	0.39796		
		Al3: 1f	(0.50000, 0.50000, 0.00000)	0.39339		
		Al4: 2l	(0.24675, 0.50000, 0.50000)			
		Zn: 1e	(0.00000, 0.50000, 0.00000)			
		Ti: 2i	(0.25277, 0.00000, 0.00000)			
7 ($(\text{Al}_{0.667}\text{Zn}_{0.333})_3\text{Ti}$)	$P4/mmm$ (123)	Al1: 2f	(0.00000, 0.50000, 0.00000)	0.39469		-0.088519
		Al2: 2h	(0.50000, 0.50000, 0.25868)			
		Zn: 2e	(0.00000, 0.50000, 0.50000)	0.79108		
		Ti: 2g	(0.00000, 0.00000, 0.24455)			
8 ($(\text{Al}_{0.5}\text{Zn}_{0.5})_3\text{Ti}$)	$P4nm$ (99)	Al1: 1b	(0.50000, 0.50000, 0.99148)	0.39483		-0.086114
		Al2: 2h	(0.50000, 0.50000, 0.25868)			
		Zn1: 1b	(0.50000, 0.50000, 0.50445)	0.78682		
		Zn2: 2c	(0.00000, 0.50000, 0.74662)			
		Ti1: 1a	(0.00000, 0.00000, 0.49545)			
		Ti2: 1a	(0.00000, 0.00000, 0.00730)			
10 ($(\text{Al}_{0.333}\text{Zn}_{0.667})_3\text{Ti}$)	$P4/mmm$ (123)	Al: 2e	(0.00000, 0.50000, 0.50000)	0.39538		-0.071437
		Zn1: 2f	(0.00000, 0.50000, 0.00000)			
		Zn2: 2h	(0.50000, 0.50000, 0.75393)	0.77923		
		Ti: 2g	(0.00000, 0.00000, 0.74449)			
12 ($(\text{Al}_{0.667}\text{Zn}_{0.333})_3\text{Ti}$)	$P4_2/mmc$ (131)	Al1: 2c	(0.50000, 0.00000, 0.50000)	0.39323		-0.092750
		Al2: 2f	(0.50000, 0.50000, 0.25000)			
		Zn: 2d	(0.00000, 0.50000, 0.50000)	0.79569		

Structure ID (Composition)	Space Group (#)	Wyckoff position Site (x, y, z)	$a/b/c$ (nm)	$\alpha/\beta/\gamma$	ΔE_f (eV/atom)
16 $((\text{Al}_{0.333}\text{Zn}_{0.667})_3\text{Ti})$	$P4_2/mmc$ (131)	Ti: $2e$ (0.00000, 0.00000, 0.25000)			
		Al: $2c$ (0.50000, 0.00000, 0.50000)	0.39343		-0.083724
		Zn1: $2d$ (0.00000, 0.50000, 0.50000)			
		Zn2: $2f$ (0.50000, 0.50000, 0.25000)	0.78425		
17 $((\text{Al}_{0.167}\text{Zn}_{0.833})_3\text{Ti})$	$Pmnm$ (47)	Ti: $2e$ (0.00000, 0.00000, 0.25000)			
		Al: $1d$ (0.50000, 0.00000, 0.50000)	0.78322		-0.043796
		Zn1: $1c$ (0.00000, 0.00000, 0.50000)	0.39620		
		Zn2: $1e$ (0.00000, 0.50000, 0.00000)	0.39049		
		Zn3: $1f$ (0.50000, 0.50000, 0.00000)			
		Zn4: $2l$ (0.24904, 0.50000, 0.50000)			
18 $((\text{Al}_{0.167}\text{Zn}_{0.833})_3\text{Ti})$	$P4/mnm$ (123)	Ti: $2i$ (0.25294, 0.00000, 0.00000)			
		Al: $1c$ (0.50000, 0.50000, 0.00000)	0.39057		-0.042647
		Zn1: $1d$ (0.50000, 0.50000, 0.50000)			
		Zn2: $4i$ (0.00000, 0.50000, 0.74806)	0.79395		
		Ti1: $1a$ (0.50000, 0.00000, 0.00000)			
19 $((\text{Al}_{0.833}\text{Zn}_{0.167})_3\text{Ti})$	$I4/mmm$ (139)	Ti2: $1b$ (0.00000, 0.00000, 0.50000)			
		Al1: $2a$ (0.00000, 0.00000, 0.00000)	0.56249		-0.052648
		Al2: $8f$ (0.25000, 0.25000, 0.25000)			
		Zn: $2b$ (0.00000, 0.00000, 0.50000)	0.78638		
		Ti: $4c$ (0.00000, 0.50000, 0.00000)			
22 $((\text{Al}_{0.5}\text{Zn}_{0.5})_3\text{Ti})$	$Fmmm$ (69)	Al1: $4a$ (0.00000, 0.00000, 0.00000)	0.78866		-0.097209
		Al2: $8d$ (0.25000, 0.50000, 0.25000)	0.77980		
		Zn1: $4b$ (0.50000, 0.50000, 0.50000)	0.79469		
		Zn2: $8e$ (0.25000, 0.25000, 0.00000)			
		Ti: $8c$ (0.00000, 0.25000, 0.25000)			
24 $((\text{Al}_{0.167}\text{Zn}_{0.833})_3\text{Ti})$	$I4/mmm$ (139)	Al: $2a$ (0.00000, 0.00000, 0.00000)	0.55276		-0.047007
		Zn1: $2b$ (0.00000, 0.00000, 0.50000)			
		Zn2: $8f$ (0.25000, 0.25000, 0.25000)	0.79260		
		Ti: $4c$ (0.50000, 0.00000, 0.00000)			
25 $((\text{Al}_{0.333}\text{Zn}_{0.667})_3\text{Ti})$	$P4/mmm$ (123)	Al1: $1c$ (0.50000, 0.50000, 0.00000)	0.56278		-0.055676
		Al2: $4k$ (0.24866, 0.24866, 0.50000)			
		Zn: $1a$ (0.00000, 0.00000, 0.00000)	0.39286		
		Ti: $2f$ (0.00000, 0.50000, 0.00000)			
26 $((\text{Al}_{0.667}\text{Zn}_{0.333})_3\text{Ti})$	$Cmmm$ (65)	Al1: $2d$ (0.00000, 0.00000, 0.50000)	0.79601		-0.055190
		Al2: $4f$ (0.25000, 0.25000, 0.50000)	0.78596		
		Al3: $4i$ (0.50000, 0.75586, 0.00000)	0.39752		
		Zn: $2c$ (0.50000, 0.00000, 0.50000)			
		Ti: $4g$ (0.24359, 0.00000, 0.00000)			
30 $((\text{Al}_{0.5}\text{Zn}_{0.5})_3\text{Ti})$	$Cmmm$ (65)	Al1: $2d$ (0.00000, 0.00000, 0.50000)	0.79449		-0.099640
		Al2: $4f$ (0.25000, 0.25000, 0.50000)	0.78858		
		Zn1: $2c$ (0.50000, 0.00000, 0.50000)	0.38992		
		Zn2: $4i$ (0.50000, 0.75411, 0.00000)			
		Ti: $4g$ (0.24546, 0.00000, 0.00000)			
31 $((\text{Al}_{0.333}\text{Zn}_{0.667})_3\text{Ti})$	$Pmma$ (51)	Al: $2b$ (0.00000, 0.50000, 0.00000)	0.55906		-0.082515
		Zn1: $2d$ (0.00000, 0.50000, 0.50000)	0.38992		
		Zn2: $2e$ (0.25000, 0.00000, 0.74304)	0.55737		
		Ti: $2e$ (0.24546, 0.00000, 0.00000)			
33 $((\text{Al}_{0.5}\text{Zn}_{0.5})_3\text{Ti})$	$Cmmm$ (65)	Al1: $2c$ (0.50000, 0.00000, 0.50000)	0.78812		-0.100943
		Al2: $4g$ (0.24514, 0.00000, 0.00000)	0.78084		
		Zn1: $2d$ (0.00000, 0.00000, 0.50000)	0.39734		
		Zn2: $4f$ (0.25000, 0.75000, 0.50000)			
		Ti: $4i$ (0.50000, 0.75493, 0.00000)			
34 $((\text{Al}_{0.333}\text{Zn}_{0.667})_3\text{Ti})$	$Amm2$ (38)	Al1: $2a$ (0.00000, 0.00000, 0.99549)	0.39442		-0.082264
		Al2: $2b$ (0.50000, 0.00000, 0.25439)	0.78129		
		Zn1: $2a$ (0.00000, 0.00000, 0.50329)	0.78863		
		Zn2: $2b$ (0.50000, 0.00000, 0.74742)			
		Zn3: $4e$ (0.50000, 0.75092, 0.50031)			
35 $((\text{Al}_{0.167}\text{Zn}_{0.833})_3\text{Ti})$	$Cmmm$ (65)	Ti: $4d$ (0.00000, 0.75405, 0.24939)			
		Al: $2c$ (0.50000, 0.00000, 0.50000)	0.79345		-0.047135
		Zn1: $2d$ (0.00000, 0.00000, 0.50000)	0.78131		
		Zn2: $4f$ (0.25000, 0.75000, 0.50000)	0.39152		
		Zn3: $4g$ (0.24733, 0.00000, 0.00000)			

Structure ID (Composition)	Space Group (#)	Wyckoff position Site (x, y, z)	a/b/c (nm)	$\alpha/\beta/\gamma$	ΔE_f (eV/atom)
36 $((\text{Al}_{0.167}\text{Zn}_{0.833})_3\text{Ti})$	$P4/mmm$ (123)	Ti: 4 <i>i</i> (0.50000, 0.75364, 0.00000) Al: 1 <i>a</i> (0.00000, 0.00000, 0.00000) Zn1: 1 <i>c</i> (0.50000, 0.50000, 0.00000) Zn2: 4 <i>k</i> (0.25162, 0.25162, 0.50000) Ti: 2 <i>f</i> (0.50000, 0.00000, 0.00000)	0.55266		-0.045109
37 $((\text{Al}_{0.889}\text{Zn}_{0.111})_3\text{Ti})$	$P4/mmm$ (123)	Al1: 2 <i>f</i> (0.00000, 0.50000, 0.00000) Al2: 2 <i>h</i> (0.50000, 0.50000, 0.83284) Al3: 4 <i>i</i> (0.00000, 0.50000, 0.66307) Zn: 1 <i>d</i> (0.50000, 0.50000, 0.50000) Ti1: 1 <i>b</i> (0.00000, 0.00000, 0.50000) Ti2: 2 <i>g</i> (0.00000, 0.00000, 0.83159)	0.39780	1.18382	-0.033494
75 $((\text{Al}_{0.333}\text{Zn}_{0.667})_3\text{Ti})$	$P4/mmm$ (123)	Al1: 1 <i>d</i> (0.50000, 0.50000, 0.50000) Al2: 2 <i>f</i> (0.00000, 0.50000, 0.00000) Zn1: 2 <i>h</i> (0.50000, 0.50000, 0.00000) Zn2: 4 <i>i</i> (0.00000, 0.50000, 0.66852) Ti1: 1 <i>b</i> (0.00000, 0.00000, 0.50000) Ti2: 2 <i>g</i> (0.00000, 0.00000, 0.83802)	0.39406		-0.076372
78 $((\text{Al}_{0.667}\text{Zn}_{0.333})_3\text{Ti})$	$Pmmm$ (47)	Al1: 1 <i>b</i> (0.50000, 0.00000, 0.00000) Al2: 1 <i>h</i> (0.50000, 0.50000, 0.50000) Al3: 2 <i>n</i> (0.00000, 0.33316, 0.50000) Al4: 2 <i>p</i> (0.50000, 0.83329, 0.50000) Zn1: 1 <i>c</i> (0.00000, 0.00000, 0.50000) Zn2: 2 <i>o</i> (0.50000, 0.33358, 0.00000) Ti1: 1 <i>e</i> (0.00000, 0.50000, 0.00000) Ti2: 2 <i>m</i> (0.00000, 0.83339, 0.00000)	0.39471		-0.091997
101 $((\text{Al}_{0.222}\text{Zn}_{0.778})_3\text{Ti})$	$Pmmm$ (47)	Al1: 1 <i>c</i> (0.00000, 0.00000, 0.50000) Al2: 1 <i>h</i> (0.50000, 0.50000, 0.50000) Zn1: 1 <i>b</i> (0.50000, 0.00000, 0.00000) Zn2: 2 <i>n</i> (0.00000, 0.33165, 0.50000) Zn3: 2 <i>o</i> (0.50000, 0.33114, 0.00000) Zn4: 2 <i>p</i> (0.50000, 0.16812, 0.50000) Ti1: 1 <i>e</i> (0.00000, 0.50000, 0.00000) Ti2: 2 <i>m</i> (0.00000, 0.16413, 0.00000)	0.39406		-0.058077
105 $((\text{Al}_{0.889}\text{Zn}_{0.111})_3\text{Ti})$	$C2/m$ (12)	Al1: 4 <i>f</i> (0.25000, 0.25000, 0.50000) Al2: 4 <i>i</i> (0.83464, 0.50000, 0.16677) Al3: 8 <i>j</i> (0.08237, 0.24888, 0.16892) Zn: 2 <i>c</i> (0.00000, 0.00000, 0.50000) Ti1: 2 <i>d</i> (0.00000, 0.50000, 0.50000) Ti2: 4 <i>i</i> (0.33192, 0.50000, 0.16354)	0.96971	0.56289	89.555
132 $((\text{Al}_{0.222}\text{Zn}_{0.778})_3\text{Ti})$	$C2$ (5)	Al: 4 <i>c</i> (0.08534, 0.41673, 0.16932) Zn1: 2 <i>b</i> (0.00000, 0.16235, 0.50000) Zn2: 4 <i>c</i> (0.08276, 0.91524, 0.16842) Zn3: 4 <i>c</i> (0.25218, 0.41782, 0.50026) Zn4: 4 <i>c</i> (0.83378, 0.66856, 0.16788) Ti1: 2 <i>b</i> (0.00000, 0.66030, 0.50000) Ti2: 4 <i>c</i> (0.83476, 0.17033, 0.16439)	0.95996	0.55681	89.502
133 $((\text{Al}_{0.333}\text{Zn}_{0.667})_3\text{Ti})$	$P\bar{3}m1$ (164)	Al: 3 <i>f</i> (0.50000, 0.00000, 0.50000) Zn: 6 <i>i</i> (0.66618, 0.83309, 0.16189) Ti1: 1 <i>b</i> (0.00000, 0.00000, 0.50000) Ti2: 2 <i>d</i> (0.66667, 0.33333, 0.17444)	0.55759		-0.072397
135 $((\text{Al}_{0.222}\text{Zn}_{0.778})_3\text{Ti})$	$C2/m$ (12)	Al: 4 <i>i</i> (0.16633, 0.50000, 0.16823) Zn1: 2 <i>c</i> (0.00000, 0.00000, 0.50000) Zn2: 4 <i>f</i> (0.25000, 0.25000, 0.50000) Zn3: 8 <i>j</i> (0.91698, 0.75065, 0.16754) Ti1: 2 <i>d</i> (0.00000, 0.50000, 0.50000) Ti2: 4 <i>i</i> (0.66801, 0.50000, 0.16485)	0.96752	0.55250	89.069
136 $((\text{Al}_{0.111}\text{Zn}_{0.889})_3\text{Ti})$	$C2/m$ (12)	Al: 2 <i>d</i> (0.00000, 0.50000, 0.50000) Zn1: 4 <i>f</i> (0.25000, 0.25000, 0.50000) Zn2: 4 <i>i</i> (0.33255, 0.50000, 0.83593) Zn3: 8 <i>j</i> (0.08408, 0.24871, 0.83501) Ti1: 2 <i>c</i> (0.00000, 0.00000, 0.50000) Ti2: 4 <i>i</i> (0.83517, 0.50000, 0.83131)	0.96614	0.55303	89.386

Structure ID (Composition)	Space Group (#)	Wyckoff position	$a/b/c$ (nm)	$\alpha/\beta/\gamma$	ΔE_f (eV/atom)
		Site (x, y, z)			
137 $((\text{Al}_{0.889}\text{Zn}_{0.111})_3\text{Ti})$	$Cmmm$ (65)	Al1: $4f$ (0.25000, 0.75000, 0.50000) Al2: $4g$ (0.66595, 0.00000, 0.00000) Al3: $8q$ (0.58266, 0.74863, 0.50000) Zn: $2a$ (0.00000, 0.00000, 0.00000) Ti1: $2b$ (0.50000, 0.00000, 0.00000) Ti2: $4g$ (0.16730, 0.00000, 0.00000)	1.68703		-0.037603
144 $((\text{Al}_{0.778}\text{Zn}_{0.222})_3\text{Ti})$	$P2/m$ (10)	Al1: $1b$ (0.25000, 0.75000, 0.50000) Al2: $2m$ (0.16562, 0.00000, 0.33882) Al3: $2n$ (0.33605, 0.50000, 0.16661) Al4: $2n$ (0.33224, 0.50000, 0.66934) Zn1: $1d$ (0.50000, 0.00000, 0.00000) Zn2: $1f$ (0.00000, 0.50000, 0.50000) Ti1: $1g$ (0.50000, 0.00000, 0.50000) Ti2: $2m$ (0.16708, 0.00000, 0.84053)	0.88328	107.965	-0.069273
169 $((\text{Al}_{0.556}\text{Zn}_{0.444})_3\text{Ti})$	$P2/m$ (10)	Al1: $1b$ (0.00000, 0.50000, 0.00000) Al2: $1d$ (0.50000, 0.00000, 0.00000) Al3: $1f$ (0.00000, 0.50000, 0.50000) Al4: $2n$ (0.66693, 0.50000, 0.33974) Zn1: $2m$ (0.83347, 0.00000, 0.67204) Zn2: $2n$ (0.66811, 0.50000, 0.83433) Ti1: $1g$ (0.50000, 0.00000, 0.50000) Ti2: $2m$ (0.83293, 0.00000, 0.17203)	0.87961	107.848	-0.099920
172 $((\text{Al}_{0.833}\text{Zn}_{0.167})_3\text{Ti})$	$P2/m$ (10)	Al1: $1f$ (0.00000, 0.50000, 0.50000) Al2: $2n$ (0.66343, 0.50000, 0.33224) Zn1: $1b$ (0.00000, 0.50000, 0.00000) Zn2: $1d$ (0.50000, 0.00000, 0.00000) Zn3: $2m$ (0.83328, 0.00000, 0.67499) Zn4: $2n$ (0.66906, 0.50000, 0.83549) Ti1: $1g$ (0.50000, 0.00000, 0.50000) Ti2: $2m$ (0.83315, 0.00000, 0.17630)	0.88036	108.082	-0.083326
180 $((\text{Al}_{0.444}\text{Zn}_{0.556})_3\text{Ti})$	$Amm2$ (38)	Al1: $4d$ (0.00000, 0.33290, 0.50633) Al2: $4e$ (0.50000, 0.08332, 0.74514) Zn1: $2a$ (0.00000, 0.00000, 0.48999) Zn2: $4e$ (0.50000, 0.91733, 0.25014) Zn3: $4e$ (0.50000, 0.24946, 0.25282) Ti1: $2a$ (0.00000, 0.00000, 0.98960) Ti2: $4d$ (0.00000, 0.16664, 0.50577)	0.39443		-0.096553
182 $((\text{Al}_{0.222}\text{Zn}_{0.778})_3\text{Ti})$	$Amm2$ (38)	Al: $4d$ (0.50000, 0.08466, 0.75062) Zn1: $2a$ (0.00000, 0.00000, 0.49129) Zn2: $4d$ (0.00000, 0.33207, 0.50430) Zn3: $4e$ (0.50000, 0.91670, 0.24931) Zn4: $4e$ (0.50000, 0.24897, 0.25094) Ti1: $2a$ (0.00000, 0.00000, 0.98934) Ti2: $4d$ (0.00000, 0.16569, 0.50451)	0.39037		-0.059509
187 $((\text{Al}_{0.444}\text{Zn}_{0.556})_3\text{Ti})$	$P2/m$ (10)	Al1: $2m$ (0.83436, 0.00000, 0.67155) Al2: $2n$ (0.66363, 0.50000, 0.32741) Zn1: $1b$ (0.00000, 0.50000, 0.00000) Zn2: $1d$ (0.50000, 0.00000, 0.00000) Zn3: $1f$ (0.00000, 0.50000, 0.50000) Zn4: $2n$ (0.66723, 0.50000, 0.83489) Ti1: $1g$ (0.50000, 0.00000, 0.50000) Ti2: $2m$ (0.83306, 0.00000, 0.17108)	0.87549	107.885	-0.097267
200 $((\text{Al}_{0.222}\text{Zn}_{0.778})_3\text{Ti})$	$Cmmm$ (65)	Al: $4f$ (0.25000, 0.75000, 0.25000) Zn1: $2a$ (0.00000, 0.00000, 0.00000) Zn2: $4g$ (0.66463, 0.00000, 0.00000) Zn3: $8q$ (0.58272, 0.74981, 0.50000) Ti1: $2b$ (0.50000, 0.00000, 0.00000) Ti2: $4g$ (0.16908, 0.00000, 0.00000)	1.67295		-0.054539
201 $((\text{Al}_{0.222}\text{Zn}_{0.778})_3\text{Ti})$	$P2/m$ (10)	Al1: $1b$ (0.00000, 0.50000, 0.00000) Al2: $1d$ (0.50000, 0.00000, 0.00000) Zn1: $1f$ (0.00000, 0.50000, 0.50000) Zn2: $2m$ (0.16672, 0.00000, 0.33761)	0.87467	107.988	-0.060235

Structure ID (Composition)	Space Group (#)	Wyckoff position Site (x, y, z)	$a/b/c$ (nm)	$\alpha/\beta/\gamma$	ΔE_f (eV/atom)
430 $((\text{Al}_{0.778}\text{Zn}_{0.222})_3\text{Ti})$	$Pmmm$ (47)	Zn3: $2n$ (0.33348, 0.50000, 0.16948)			
		Zn4: $2n$ (0.33243, 0.50000, 0.66468)			
		Ti1: $1g$ (0.50000, 0.00000, 0.50000)			
		Ti2: $2m$ (0.16674, 0.00000, 0.83773)			
		Al1: $1d$ (0.50000, 0.00000, 0.50000)	1.59128		-0.091826
		Al2: $1e$ (0.00000, 0.50000, 0.00000)	0.39545		
		Al3: $2j$ (0.75013, 0.00000, 0.50000)	0.39106		
		Al4: $2l$ (0.62499, 0.50000, 0.50000)			
		Al5: $2l$ (0.87495, 0.50000, 0.50000)			
		Zn1: $1c$ (0.00000, 0.00000, 0.50000)			
		Zn2: $1f$ (0.50000, 0.50000, 0.00000)			
		Zn3: $2k$ (0.74982, 0.50000, 0.00000)			
		Ti1: $2i$ (0.62504, 0.00000, 0.00000)			
		Ti2: $2i$ (0.87505, 0.00000, 0.00000)			
1091 $((\text{Al}_{0.833}\text{Zn}_{0.167})_3\text{Ti})$	$Cmca$ (64)	Al1: $4a$ (0.50000, 0.00000, 0.50000)	0.79569		-0.054075
		Al2: $8e$ (0.75000, 0.12254, 0.25000)	1.11833		
		Al3: $8f$ (0.50000, 0.24827, 0.00194)	0.55960		
		Zn: $4b$ (0.50000, 0.00000, 0.00000)			
		Ti: $8e$ (0.75000, 0.12783, 0.75000)			
1297 $((\text{Al}_{0.167}\text{Zn}_{0.833})_3\text{Ti})$	$Cmca$ (64)	Al: $4b$ (0.00000, 0.00000, 0.50000)	0.78119		-0.046601
		Zn1: $4a$ (0.00000, 0.00000, 0.00000)	1.11433		
		Zn2: $8e$ (0.25000, 0.87314, 0.25000)	0.55690		
		Zn3: $8f$ (0.50000, 0.24958, 0.50092)			
		Ti: $8e$ (0.25000, 0.87704, 0.75000)			
1635 $((\text{Al}_{0.917}\text{Zn}_{0.083})_3\text{Ti})$	$I4/mmm$ (139)	Al1: $2b$ (0.00000, 0.00000, 0.50000)	0.79569		-0.028708
		Al2: $4c$ (0.00000, 0.50000, 0.00000)			
		Al3: $16n$ (0.25086, 0.50000, 0.25277)	0.79063		
		Zn: $2a$ (0.00000, 0.00000, 0.00000)			
		Ti: $8h$ (0.24868, 0.24868, 0.50000)			
1689 $((\text{Al}_{0.417}\text{Zn}_{0.167})_3\text{Ti})$	$Immm$ (71)	Al1: $2d$ (0.00000, 0.50000, 0.00000)	0.79461		-0.095250
		Al2: $8n$ (0.75270, 0.25270, 0.50000)	0.78472		
		Zn1: $2a$ (0.00000, 0.00000, 0.00000)	0.78091		
		Zn2: $2b$ (0.50000, 0.00000, 0.00000)			
		Zn3: $2c$ (0.00000, 0.00000, 0.50000)			
1705 $((\text{Al}_{0.083}\text{Zn}_{0.917})_3\text{Ti})$	$I4/mmm$ (139)	Zn4: $8l$ (0.00000, 0.24796, 0.75003)			
		Ti: $8m$ (0.25215, 0.00000, 0.74732)			
		Al: $2b$ (0.00000, 0.00000, 0.50000)	0.78292		-0.023288
		Zn1: $2a$ (0.00000, 0.00000, 0.00000)			
		Zn2: $4c$ (0.00000, 0.50000, 0.00000)	0.79008		
2078 $((\text{Al}_{0.25}\text{Zn}_{0.75})_3\text{Ti})$	$Cmmm$ (65)	Zn3: $16n$ (0.50000, 0.75114, 0.25186)			
		Ti: $8h$ (0.75206, 0.24793, 0.50000)			
		Al: $2a$ (0.00000, 0.00000, 0.00000)	1.58124		-0.066126
		Al2: $4h$ (0.62523, 0.00000, 0.50000)	0.78116		
		Zn1: $2b$ (0.50000, 0.00000, 0.00000)	0.39273		
		Zn2: $4f$ (0.25000, 0.75000, 0.50000)			
		Zn3: $4g$ (0.75000, 0.00000, 0.00000)			
1 (Zn_3Ti)	$Pm\bar{3}m$ (221)	Zn4: $4h$ (0.87452, 0.00000, 0.50000)			
		Zn5: $4j$ (0.50000, 0.25007, 0.50000)			
		Ti: $8p$ (0.75206, 0.24793, 0.50000)			
1 (Zn_3Ti)	$Pm\bar{3}m$ (221)	Zn: $3c$ (0.50000, 0.50000, 0.00000)	0.39254		0.0
		Ti: $1a$ (0.00000, 0.00000, 0.00000)			

TABLE VI: Description of structures used in cluster-expansion fits to calculate the formation energy of $DO_{22}-(Al_{1-x}Zn_x)_3Ti$. Here, the formation energies (ΔE_f) are relative to $DO_{22}-Al_3Ti$ and $DO_{22}-Zn_3Ti$.

Structure ID (Composition)	Space Group (#)	Wyckoff position Site (x, y, z)	$a/b/c$ (nm)	$\alpha/\beta/\gamma$	ΔE_f (eV/atom)
0 (Al_3Ti)	$I\bar{4}/mmm$ (139)	Al1: $2b$ (0.00000, 0.00000, 0.50000) Al2: $4d$ (0.00000, 0.50000, 0.25000) Ti: $2a$ (0.00000, 0.00000, 0.00000)	0.38443		0.0
2 ($(Al_{0.833}Zn_{0.167})_3Ti$)	$P4/mmm$ (123)	Al1: $1c$ (0.50000, 0.50000, 0.00000) Al2: $4i$ (0.50000, 0.00000, 0.74891) Zn: $1b$ (0.00000, 0.00000, 0.50000) Ti1: $1a$ (0.00000, 0.00000, 0.00000) Ti2: $1d$ (0.50000, 0.50000, 0.50000)	0.38539		0.020019
3 ($(Al_{0.667}Zn_{0.333})_3Ti$)	$I4/mmm$ (139)	Al: $4d$ (0.00000, 0.50000, 0.25000) Zn: $2b$ (0.00000, 0.00000, 0.50000) Ti: $2a$ (0.00000, 0.00000, 0.00000)	0.38621		0.048280
4 ($(Al_{0.833}Zn_{0.167})_3Ti$)	$P4/mmm$ (123)	Al1: $1a$ (0.00000, 0.00000, 0.00000) Al2: $1b$ (0.50000, 0.50000, 0.00000) Al3: $1c$ (0.50000, 0.50000, 0.50000) Al4: $2g$ (0.00000, 0.50000, 0.25767) Zn: $1d$ (0.00000, 0.00000, 0.50000) Ti: $2g$ (0.00000, 0.50000, 0.75198)	0.38322		0.005135
6 ($(Al_{0.5}Zn_{0.5})_3Ti$)	$P\bar{4}m2$ (115)	Al1: $1a$ (0.00000, 0.00000, 0.00000) Al2: $1b$ (0.50000, 0.50000, 0.00000) Al3: $1d$ (0.00000, 0.00000, 0.50000) Zn1: $1c$ (0.50000, 0.50000, 0.50000) Zn2: $2g$ (0.50000, 0.00000, 0.26171) Ti: $2g$ (0.50000, 0.00000, 0.74831)	0.38725		0.062123
7 ($(Al_{0.667}Zn_{0.333})_3Ti$)	$P4/nmm$ (129)	Al1: $2a$ (0.25000, 0.75000, 0.00000) Al2: $2c$ (0.25000, 0.25000, 0.26492) Zn: $2b$ (0.25000, 0.75000, 0.50000) Ti: $2c$ (0.25000, 0.25000, 0.74836)	0.38562		0.006048
9 ($(Al_{0.333}Zn_{0.667})_3Ti$)	$P4/nmm$ (129)	Al: $2a$ (0.25000, 0.75000, 0.00000) Zn1: $2b$ (0.25000, 0.75000, 0.50000) Zn2: $2c$ (0.25000, 0.75000, 0.73168) Ti: $2c$ (0.25000, 0.25000, 0.26074)	0.39248		0.033561
10 ($(Al_{0.667}Zn_{0.333})_3Ti$)	$I\bar{4}m2$ (119)	Al1: $2b$ (0.00000, 0.00000, 0.50000) Al2: $2c$ (0.00000, 0.50000, 0.25000) Zn: $2d$ (0.50000, 0.00000, 0.25000) Ti: $2a$ (0.00000, 0.00000, 0.00000)	0.38281		0.016087
11 ($(Al_{0.5}Zn_{0.5})_3Ti$)	$P\bar{4}m2$ (115)	Al1: $1b$ (0.50000, 0.50000, 0.00000) Al2: $2g$ (0.00000, 0.50000, 0.25217) Zn1: $1d$ (0.00000, 0.00000, 0.50000) Zn2: $2g$ (0.00000, 0.50000, 0.74964) Ti1: $1a$ (0.00000, 0.00000, 0.00000) Ti2: $1c$ (0.50000, 0.50000, 0.50000)	0.38581		0.047775
12 ($(Al_{0.333}Zn_{0.667})_3Ti$)	$I\bar{4}m2$ (119)	Al: $2d$ (0.50000, 0.00000, 0.25000) Zn1: $2b$ (0.00000, 0.00000, 0.50000) Zn2: $2c$ (0.00000, 0.50000, 0.25000) Ti: $2a$ (0.00000, 0.00000, 0.00000)	0.39088		0.073735
13 ($(Al_{0.667}Zn_{0.333})_3Ti$)	$P4_2/mmc$ (131)	Al1: $2c$ (0.00000, 0.50000, 0.00000) Al2: $2f$ (0.50000, 0.50000, 0.25000) Zn: $2e$ (0.00000, 0.00000, 0.25000) Ti: $2d$ (0.00000, 0.50000, 0.50000)	0.38291		0.016289
14 ($(Al_{0.5}Zn_{0.5})_3Ti$)	$Pmmm$ (47)	Al1: $1g$ (0.00000, 0.50000, 0.50000) Al2: $2j$ (0.25218, 0.00000, 0.00000) Zn1: $1b$ (0.50000, 0.00000, 0.00000) Zn2: $2k$ (0.25047, 0.50000, 0.00000) Ti1: $1a$ (0.00000, 0.00000, 0.00000) Ti2: $1h$ (0.50000, 0.50000, 0.50000)	0.84635 0.38733 0.38505		0.047411
15 ($(Al_{0.667}Zn_{0.333})_3Ti$)	$P4_2/mmc$ (131)	Al1: $2e$ (0.00000, 0.00000, 0.25000) Al2: $2d$ (0.50000, 0.00000, 0.00000) Zn: $2f$ (0.50000, 0.50000, 0.25000)	0.39084 0.82667		0.071275

Structure ID (Composition)	Space Group (#)	Wyckoff position Site (x, y, z)	$a/b/c$ (nm)	$\alpha/\beta/\gamma$	ΔE_f (eV/atom)
16 $((\text{Al}_{0.5}\text{Zn}_{0.5})_3\text{Ti})$	$P\bar{4}m2$ (115)	Ti: $2c$ (0.50000, 0.00000, 0.50000) Al1: $1c$ (0.50000, 0.50000, 0.50000) Al2: $2g$ (0.00000, 0.50000, 0.24276) Zn1: $1a$ (0.00000, 0.00000, 0.00000) Zn2: $1b$ (0.50000, 0.50000, 0.00000) Zn3: $1d$ (0.00000, 0.00000, 0.50000) Ti: $2g$ (0.50000, 0.00000, 0.24496)	0.38619		0.013879
17 $((\text{Al}_{0.333}\text{Zn}_{0.667})_3\text{Ti})$	$Pmm2$ (25)	Al1: $1c$ (0.50000, 0.00000, 0.25377) Al2: $1d$ (0.50000, 0.50000, 0.99495) Zn1: $1a$ (0.00000, 0.00000, 0.50637) Zn2: $1b$ (0.00000, 0.50000, 0.25214) Zn3: $1b$ (0.00000, 0.50000, 0.74704) Zn4: $1c$ (0.50000, 0.00000, 0.74694) Ti1: $1a$ (0.00000, 0.00000, 0.99072) Ti2: $1d$ (0.50000, 0.50000, 0.50807)	0.39062 0.39159 0.81703		0.030307
19 $((\text{Al}_{0.333}\text{Zn}_{0.667})_3\text{Ti})$	$I4/mmm$ (139)	Al: $2b$ (0.00000, 0.00000, 0.50000) Zn: $4d$ (0.00000, 0.50000, 0.25000) Ti: $2a$ (0.00000, 0.00000, 0.00000)	0.38996		0.005666
373 $((\text{Al}_{0.167}\text{Zn}_{0.833})_3\text{Ti})$	$Pmnm$ (59)	Al: $2b$ (0.25000, 0.12699, 0.75000) Zn1: $2b$ (0.25000, 0.62352, 0.75000) Zn2: $4f$ (0.49567, 0.62426, 0.25000) Zn3: $4f$ (0.50382, 0.12639, 0.25000) Ti1: $2a$ (0.25000, 0.36909, 0.25000) Ti2: $2a$ (0.25000, 0.88202, 0.25000)	0.78294 0.79426 0.39613		0.002721
376 $((\text{Al}_{0.833}\text{Zn}_{0.167})_3\text{Ti})$	$I4_1/amd$ (141)	Al1: $4b$ (0.00000, 0.25000, 0.37500) Al2: $16f$ (0.24965, 0.50000, 0.00000) Zn: $4a$ (0.00000, 0.25000, 0.87500) Ti: $8e$ (0.00000, 0.25000, 0.12440)	0.54461		0.015260
396 $((\text{Al}_{0.667}\text{Zn}_{0.333})_3\text{Ti})$	$Imma$ (74)	Al1: $4b$ (0.00000, 0.00000, 0.50000) Al2: $4e$ (0.00000, 0.25000, 0.00662) Al3: $8g$ (0.25000, 0.62489, 0.25000) Zn: $8g$ (0.25000, 0.37489, 0.25000) Ti1: $4a$ (0.00000, 0.00000, 0.00000) Ti2: $4e$ (0.00000, 0.25000, 0.50683)	0.54399 1.70748 0.54332		0.012183
432 $((\text{Al}_{0.583}\text{Zn}_{0.417})_3\text{Ti})$	$C2$ (5)	Al1: $2a$ (0.00000, 0.37379, 0.0000) Al2: $2a$ (0.00000, 0.87449, 0.00000) Al3: $2b$ (0.00000, 0.37475, 0.50000) Al4: $4c$ (0.25017, 0.37508, 0.24864) Al5: $4c$ (0.37278, 0.62384, 0.62147) Zn1: $2b$ (0.00000, 0.87669, 0.50000) Zn2: $4c$ (0.12702, 0.62627, 0.87589) Zn3: $4c$ (0.25000, 0.37503, 0.74771) Ti1: $4c$ (0.12396, 0.62362, 0.37304) Ti2: $4c$ (0.12607, 0.12629, 0.87777)	1.79356 0.54430 0.54396	107.601	0.034503
898 $((\text{Al}_{0.833}\text{Zn}_{0.167})_3\text{Ti})$	$C2/m$ (12)	Al: $2b$ (0.00000, 0.50000, 0.00000) Zn1: $2c$ (0.00000, 0.00000, 0.50000) Zn2: $4i$ (0.11492, 0.50000, 0.14360) Zn3: $4i$ (0.36853, 0.50000, 0.38786) Ti: $4i$ (0.73864, 0.50000, 0.77038)	1.41849 0.39591 0.86877	30.298	0.00000
1011 $((\text{Al}_{0.833}\text{Zn}_{0.167})_3\text{Ti})$	$P4/mmm$ (129)	Al1: $2b$ (0.25000, 0.75000, 0.50000) Al2: $2c$ (0.25000, 0.25000, 0.11588) Al3: $2c$ (0.25000, 0.25000, 0.62624) Al4: $4f$ (0.25000, 0.75000, 0.24783) Zn: $2a$ (0.25000, 0.75000, 0.00000) Ti1: $2c$ (0.25000, 0.25000, 0.37411) Ti2: $2c$ (0.25000, 0.25000, 0.87641)	0.38492 1.71209		0.003981
1121 $((\text{Al}_{0.667}\text{Zn}_{0.333})_3\text{Ti})$	$P4/mmm$ (123)	Al1: $1a$ (0.00000, 0.00000, 0.00000) Al2: $1b$ (0.00000, 0.00000, 0.50000) Al3: $2h$ (0.50000, 0.50000, 0.23920) Al4: $4i$ (0.50000, 0.00000, 0.37266) Zn: $4i$ (0.50000, 0.00000, 0.12170) Ti1: $1c$ (0.50000, 0.50000, 0.00000)	0.38575 1.69358		0.007385

Structure ID (Composition)	Space Group (#)	Wyckoff position Site (x, y, z)	$a/b/c$ (nm)	$\alpha/\beta/\gamma$	ΔE_f (eV/atom)
1300 $((\text{Al}_{0.5}\text{Zn}_{0.5})_3\text{Ti})$	$P4/nmm$ (129)	Ti2: $1d$ (0.50000, 0.50000, 0.50000)			
		Ti3: $2g$ (0.00000, 0.00000, 0.24682)			
		Al1: $2a$ (0.25000, 0.75000, 0.00000)	0.38730		0.008472
		Al2: $2c$ (0.25000, 0.25000, 0.13433)			
		Al3: $2c$ (0.25000, 0.25000, 0.62435)	1.66695		
		Zn1: $2b$ (0.25000, 0.75000, 0.50000)			
		Zn2: $4f$ (0.25000, 0.75000, 0.25311)			
		Ti1: $2c$ (0.25000, 0.25000, 0.87219)			
		Ti2: $2c$ (0.25000, 0.25000, 0.37656)			

TABLE VII: Description of structures used in cluster-expansion fits to calculate the formation energy of $DO_{23-}(Al_{1-x}Zn_x)_3Ti$. Here, the formation energies (ΔE_f) are relative to $DO_{23-}Al_3Ti$ and $DO_{23-}Zn_3Ti$.

Structure ID (Composition)	Space Group (#)	Wyckoff position Site (x, y, z)	$a/b/c$ (nm)	$\alpha/\beta/\gamma$	ΔE_f (eV/atom)
0 (Al_3Ti)	$I4/mmm$ (139)	Al1: $4c$ (0.00000, 0.50000, 0.00000) Al2: $4d$ (0.00000, 0.50000, 0.25000) Al3: $4e$ (0.00000, 0.00000, 0.37519) Ti: $4e$ (0.00000, 0.00000, 0.11875)	0.38962		0.0
2 ($(Al_{0.917}Zn_{0.083})_3Ti$)	$Pmmm$ (47)	Al1: $1d$ (0.50000, 0.00000, 0.00000) Al2: $1e$ (0.00000, 0.50000, 0.00000) Al3: $1f$ (0.50000, 0.50000, 0.00000) Al4: $2j$ (0.24937, 0.00000, 0.50000) Al5: $2k$ (0.24943, 0.50000, 0.00000) Al6: $2l$ (0.12281, 0.50000, 0.50000) Al7: $2i$ (0.37446, 0.00000, 0.00000) Zn: $1c$ (0.00000, 0.00000, 0.50000) Ti1: $2l$ (0.38219, 0.50000, 0.50000) Ti2: $2i$ (0.11992, 0.00000, 0.00000)	1.66677		-0.021102
4 ($(Al_{0.833}Zn_{0.167})_3Ti$)	$Immm$ (71)	Al1: $2d$ (0.00000, 0.50000, 0.00000) Al2: $4e$ (0.37655, 0.00000, 0.00000) Al3: $4f$ (0.24993, 0.00000, 0.50000) Zn: $2c$ (0.00000, 0.00000, 0.50000) Ti: $4e$ (0.11926, 0.00000, 0.00000)	1.66700		-0.038995
5 ($(Al_{0.833}Zn_{0.167})_3Ti$)	$P4_2/mmc$ (131)	Al1: $2a$ (0.00000, 0.00000, 0.00000) Al2: $2e$ (0.00000, 0.00000, 0.25000) Al3: $2f$ (0.50000, 0.50000, 0.25000) Al4: $4i$ (0.00000, 0.50000, 0.37654) Zn: $2b$ (0.50000, 0.50000, 0.00000) Ti: $4i$ (0.00000, 0.50000, 0.11925)	0.38767		-0.038480
6 ($(Al_{0.75}Zn_{0.25})_3Ti$)	$P4_2/mmc$ (131)	Al1: $1d$ (0.50000, 0.00000, 0.50000) Al2: $2i$ (0.37603, 0.00000, 0.00000) Al3: $2j$ (0.24984, 0.00000, 0.50000) Al4: $2k$ (0.24992, 0.50000, 0.00000) Al5: $2l$ (0.12078, 0.50000, 0.50000) Zn1: $1c$ (0.00000, 0.00000, 0.50000) Zn2: $1e$ (0.00000, 0.50000, 0.00000) Zn3: $1f$ (0.50000, 0.50000, 0.00000) Ti1: $2i$ (0.12047, 0.00000, 0.00000) Ti2: $2l$ (0.38121, 0.50000, 0.50000)	1.66803		-0.042754
7 ($(Al_{0.667}Zn_{0.333})_3Ti$)	$I4/mmm$ (139)	Al1: $4d$ (0.00000, 0.50000, 0.25000) Al2: $4e$ (0.00000, 0.00000, 0.37862) Zn: $4c$ (0.00000, 0.50000, 0.00000) Ti: $4e$ (0.00000, 0.00000, 0.12007)	0.38650		-0.046592
8 ($(Al_{0.917}Zn_{0.083})_3Ti$)	$P\bar{4}m2$ (115)	Al1: $1a$ (0.00000, 0.00000, 0.00000) Al2: $1b$ (0.50000, 0.50000, 0.00000) Al3: $1c$ (0.50000, 0.50000, 0.50000) Al4: $2e$ (0.00000, 0.00000, 0.25049) Al5: $2f$ (0.50000, 0.50000, 0.25041) Al6: $2g$ (0.00000, 0.50000, 0.37934) Al7: $2g$ (0.00000, 0.50000, 0.12538) Zn: $1d$ (0.00000, 0.00000, 0.50000) Ti1: $2g$ (0.00000, 0.50000, 0.63349) Ti2: $2g$ (0.00000, 0.50000, 0.86832)	0.38957		-0.005213
17 ($(Al_{0.583}Zn_{0.417})_3Ti$)	$P\bar{4}m2$ (115)	Al1: $1a$ (0.00000, 0.00000, 0.00000) Al2: $1b$ (0.50000, 0.50000, 0.00000) Al3: $1c$ (0.50000, 0.50000, 0.50000) Al4: $2g$ (0.00000, 0.50000, 0.37576) Al5: $2g$ (0.00000, 0.50000, 0.12845) Zn1: $1d$ (0.00000, 0.00000, 0.50000) Zn2: $2e$ (0.00000, 0.00000, 0.25073) Zn3: $2f$ (0.50000, 0.50000, 0.25039) Ti1: $2g$ (0.00000, 0.50000, 0.63095)	0.38690		-0.038136
			1.65762		

Structure ID (Composition)	Space Group (#)	Wyckoff position Site (x, y, z)	$a/b/c$ (nm)	$\alpha/\beta/\gamma$	ΔE_f (eV/atom)
52 $((\text{Al}_{0.667}\text{Zn}_{0.333})_3\text{Ti})$	$I4/mmm$ (139)	Ti2: $2g$ (0.00000, 0.50000, 0.86977) Al1: $4c$ (0.00000, 0.50000, 0.00000) Al2: $4e$ (0.00000, 0.00000, 0.36648) Zn: $4d$ (0.00000, 0.50000, 0.25000) Ti: $4e$ (0.00000, 0.00000, 0.11520)	0.39262		-0.017421
58 $((\text{Al}_{0.333}\text{Zn}_{0.667})_3\text{Ti})$	$I4/mmm$ (139)	Al: $4e$ (0.00000, 0.00000, 0.37023) Zn1: $4c$ (0.00000, 0.50000, 0.00000) Zn2: $4d$ (0.00000, 0.50000, 0.25000) Ti: $4e$ (0.00000, 0.00000, 0.12068)	0.39177		-0.032755
112 $((\text{Al}_{0.667}\text{Zn}_{0.333})_3\text{Ti})$	$Pmm2$ (25)	Al1: $1a$ (0.00000, 0.00000, 0.37081) Al2: $1b$ (0.00000, 0.50000, 0.50220) Al3: $1b$ (0.00000, 0.50000, 0.74737) Al4: $1b$ (0.00000, 0.50000, 0.99982) Al5: $1c$ (0.50000, 0.00000, 0.25015) Al6: $1c$ (0.50000, 0.00000, 0.50221) Al7: $1d$ (0.50000, 0.50000, 0.12768) Al8: $1d$ (0.50000, 0.50000, 0.86954) Zn1: $1a$ (0.00000, 0.00000, 0.62794) Zn2: $1b$ (0.00000, 0.50000, 0.25051) Zn3: $1c$ (0.50000, 0.00000, 0.74871) Zn4: $1c$ (0.50000, 0.00000, 0.99966) Ti1: $1a$ (0.00000, 0.00000, 0.11790) Ti2: $1a$ (0.00000, 0.00000, 0.88270) Ti3: $1d$ (0.50000, 0.50000, 0.38605) Ti4: $1d$ (0.50000, 0.50000, 0.61675)	0.39209		-0.018288
239 $((\text{Al}_{0.417}\text{Zn}_{0.593})_3\text{Ti})$	$Pmm2$ (25)	Al1: $1b$ (0.00000, 0.50000, 0.00000) Al2: $1b$ (0.00000, 0.50000, 0.74728) Al3: $1c$ (0.50000, 0.00000, 0.25261) Al4: $1d$ (0.50000, 0.50000, 0.13067) Al5: $1d$ (0.50000, 0.50000, 0.86918) Zn1: $1a$ (0.00000, 0.00000, 0.37192) Zn2: $1a$ (0.00000, 0.00000, 0.62794) Zn3: $1b$ (0.00000, 0.50000, 0.25127) Zn4: $1b$ (0.00000, 0.50000, 0.49990) Zn5: $1c$ (0.50000, 0.00000, 0.50022) Zn6: $1c$ (0.50000, 0.00000, 0.74898) Zn7: $1c$ (0.50000, 0.00000, 0.99986) Ti1: $1a$ (0.00000, 0.00000, 0.11765) Ti2: $1a$ (0.00000, 0.00000, 0.88232) Ti3: $1d$ (0.50000, 0.50000, 0.38143) Ti4: $1d$ (0.50000, 0.50000, 0.61876)	0.39127		-0.009778
275 $((\text{Al}_{0.5}\text{Zn}_{0.5})_3\text{Ti})$	$P4/mmm$ (123)	Al1: $2e$ (0.00000, 0.50000, 0.50000) Al2: $2h$ (0.50000, 0.50000, 0.13174) Zn1: $2f$ (0.00000, 0.50000, 0.00000) Zn2: $2g$ (0.00000, 0.00000, 0.36767) Zn3: $4i$ (0.00000, 0.50000, 0.25182) Ti1: $2g$ (0.00000, 0.00000, 0.12329) Ti2: $2h$ (0.50000, 0.50000, 0.38044)	0.39858		-0.025242
279 $((\text{Al}_{0.25}\text{Zn}_{0.75})_3\text{Ti})$	$Pmmm$ (47)	Al1: $1d$ (0.50000, 0.00000, 0.50000) Al2: $2l$ (0.13158, 0.50000, 0.50000) Zn1: $1c$ (0.00000, 0.00000, 0.50000) Zn2: $1e$ (0.00000, 0.50000, 0.00000) Zn3: $1f$ (0.50000, 0.50000, 0.00000) Zn4: $2i$ (0.36809, 0.00000, 0.00000) Zn5: $2j$ (0.24160, 0.00000, 0.50000) Zn6: $2k$ (0.25236, 0.50000, 0.00000) Ti1: $2i$ (0.12368, 0.00000, 0.00000) Ti2: $2l$ (0.37873, 0.50000, 0.50000)	1.53806		-0.031401
283 $((\text{Al}_{0.833}\text{Zn}_{0.167})_3\text{Ti})$	$I4mm$ (107)	Al1: $2a$ (0.00000, 0.00000, 0.62631) Al2: $4b$ (0.00000, 0.50000, 0.25184) Al3: $4b$ (0.00000, 0.50000, 0.49802) Zn: $2a$ (0.00000, 0.00000, 0.37628)	0.39104		-0.014853

Structure ID (Composition)	Space Group (#)	Wyckoff position Site (x, y, z)	a/b/c (nm)	$\alpha/\beta/\gamma$	ΔE_f (eV/atom)
355 $((\text{Al}_{0.333}\text{Zn}_{0.667})_3\text{Ti})$	<i>Imm</i> 2 (44)	Ti1: 2a (0.00000, 0.00000, 0.11600)			
		Ti2: 2a (0.00000, 0.00000, 0.88171)			
		Al1: 2a (0.00000, 0.00000, 0.63401)	0.39971		-0.024468
		Al2: 2b (0.50000, 0.00000, 0.49779)	0.39609		
		Zn1: 2a (0.00000, 0.00000, 0.36892)	1.55013		
		Zn2: 2b (0.00000, 0.50000, 0.25254)			
		Zn3: 2b (0.50000, 0.00000, 0.25083)			
		Zn4: 2b (0.00000, 0.50000, 0.49842)			
		Ti1: 2a (0.00000, 0.00000, 0.11967)			
		Ti2: 2a (0.00000, 0.00000, 0.87781)			
429 $((\text{Al}_{0.333}\text{Zn}_{0.667})_3\text{Ti})$	<i>P4/nmm</i> (129)	Al1: 2a (0.25000, 0.75000, 0.00000)	0.39386		-0.033263
		Al2: 2c (0.25000, 0.25000, 0.13191)			
		Zn1: 2b (0.25000, 0.75000, 0.50000)	1.58226		
		Zn2: 2c (0.25000, 0.25000, 0.38392)			
		Zn3: 4f (0.25000, 0.75000, 0.25922)			
		Ti1: 2c (0.25000, 0.25000, 0.61919)			
		Ti2: 2c (0.25000, 0.25000, 0.86440)			
443 $((\text{Al}_{0.333}\text{Zn}_{0.667})_3\text{Ti})$	<i>Pmnm</i> (59)	Al1: 2a (0.25000, 0.11966, 0.25000)	0.39865		-0.032402
		Al2: 2b (0.25000, 0.74379, 0.75000)	1.55615		
		Zn1: 2a (0.25000, 0.38503, 0.25000)	0.39536		
		Zn2: 2b (0.25000, 0.00052, 0.75000)			
		Zn3: 2b (0.25000, 0.25614, 0.75000)			
		Zn4: 2b (0.25000, 0.49945, 0.75000)			
		Ti1: 2a (0.25000, 0.62296, 0.25000)			
		Ti2: 2a (0.25000, 0.86427, 0.25000)			
504 $((\text{Al}_{0.417}\text{Zn}_{0.593})_3\text{Ti})$	<i>Pmm</i> 2 (25)	Al1: 1b (0.00000, 0.50000, 0.00280)	0.39577		-0.011711
		Al2: 1b (0.00000, 0.50000, 0.74714)	0.39112		
		Al3: 1c (0.50000, 0.00000, 0.25010)	1.60169		
		Al4: 1c (0.50000, 0.00000, 0.49910)			
		Al5: 1d (0.50000, 0.50000, 0.86948)			
		Zn1: 1a (0.00000, 0.00000, 0.36972)			
		Zn2: 1a (0.00000, 0.00000, 0.62785)			
		Zn3: 1b (0.00000, 0.50000, 0.25136)			
		Zn4: 1b (0.00000, 0.50000, 0.49926)			
		Zn5: 1c (0.50000, 0.00000, 0.00182)			
		Zn6: 1c (0.50000, 0.00000, 0.74893)			
		Zn7: 1d (0.50000, 0.00000, 0.12999)			
		Ti1: 1a (0.00000, 0.00000, 0.12057)			
		Ti2: 1a (0.00000, 0.00000, 0.88372)			
		Ti3: 1d (0.50000, 0.50000, 0.38135)			
		Ti4: 1d (0.50000, 0.50000, 0.61681)			
583 $((\text{Al}_{0.667}\text{Zn}_{0.333})_3\text{Ti})$	<i>I4/mmm</i> (139)	Al1: 4c (0.00000, 0.50000, 0.00000)	0.39365		-0.016714
		Al2: 4d (0.00000, 0.50000, 0.25000)			
		Zn: 4e (0.00000, 0.00000, 0.37538)	1.61934		
		Ti: 4e (0.00000, 0.00000, 0.11695)			
589 $((\text{Al}_{0.333}\text{Zn}_{0.667})_3\text{Ti})$	<i>I4/mmm</i> (139)	Al1: 4d (0.00000, 0.50000, 0.25000)	0.39104		-0.005477
		Zn1: 4c (0.00000, 0.50000, 0.00000)			
		Zn2: 4e (0.00000, 0.00000, 0.37495)	1.63020		
		Ti: 4e (0.00000, 0.00000, 0.11950)			
613 $((\text{Al}_{0.167}\text{Zn}_{0.833})_3\text{Ti})$	<i>I\bar{4}m</i> 2 (119)	Al1: 2c (0.00000, 0.50000, 0.25000)	0.39692		-0.00000
		Zn1: 2d (0.50000, 0.00000, 0.25000)			
		Zn2: 4e (0.00000, 0.00000, 0.37010)	1.56607		
		Zn3: 4f (0.50000, 0.00000, 0.00013)			
		Ti: 4e (0.00000, 0.00000, 0.12025)			
624 $((\text{Al}_{0.417}\text{Zn}_{0.593})_3\text{Ti})$	<i>P\bar{4}m</i> 2 (115)	Al1: 1b (0.50000, 0.50000, 0.00000)	0.40015		-0.017285
		Al2: 2e (0.00000, 0.00000, 0.25534)			
		Al3: 2f (0.50000, 0.50000, 0.25536)	1.54150		
		Zn1: 1a (0.00000, 0.00000, 0.00000)			
		Zn2: 1c (0.50000, 0.50000, 0.50000)			
		Zn3: 1d (0.00000, 0.00000, 0.50000)			
		Zn4: 2g (0.00000, 0.50000, 0.61449)			
		Zn5: 2g (0.00000, 0.50000, 0.87860)			

Structure ID (Composition)	Space Group (#)	Wyckoff position Site	(x, y, z)	$a/b/c$ (nm)	$\alpha/\beta/\gamma$	ΔE_f (eV/atom)
		Ti1: 2g	(0.00000, 0.50000, 0.13685)			
		Ti2: 2g	(0.00000, 0.50000, 0.37512)			

VI. ACKNOWLEDGMENTS

This research was supported by the U. S. Department of Energy, Office of Basic Energy Sciences, under Contract Nos. DE-FG02-02ER45997 (GG) and DOE-FG02-01ER45910 (AvdW and MA). Supercomputing resources were provided by the National Partnership on Advanced Computational Infrastructure (NPACI) at the University of Michigan at Ann Arbor and at the University of Illinois at Urbana-Champaign.

-
- ¹ M.Y. Drits, L.B. Ber, Y.G. Bykov, L.S. Toropova and G.K. Anastasieva, "Aging of Al-0.3 At.% Sc Alloy", *Fiz. Met. Metallof.*, Vol 57, 1984, p 1172-1179.
- ² D.N. Seidman, E.A. Marquis EA and D.C. Dunand, "Precipitation Strengthening at Ambient and Elevated Temperatures of Heat-treatable Al(Sc) Alloys", *Acta Mater.*, Vol 50, 2002, p 4021-4035.
- ³ M.S. Zedalis and M.E. Fine, "Precipitation and Ostwald Ripening in Dilute Al Base-Zr-V Alloys", *Metall. Trans. A*, Vol 17A, 1986, p 2187-2198.
- ⁴ V.R. Parameswaran, J.R. Weertman and M.E. Fine, "Coarsening Behavior of $L1_2$ Phase in an Al-Zr-Ti Alloy", *Scripta Met.*, Vol 23, 1989, p 147-150.
- ⁵ S. Fujikawa, "Solid-State Diffusion in Light Metals," *J. Jap. Inst. Light Metals*, Vol 46, 1996, p 202-215.
- ⁶ Y. Nakayama and H. Mabuchi, "Formation of Ternary $L1_2$ Compounds in Al_3Ti -Base Alloys", *Intermetallics*, Vol 1, 1993, p 41-48.
- ⁷ A. Raman and Schubert, "Über den Aufbau Einiger zu $TiAl_3$ Verwandter Legierungsreihen.I. Untersuchungen in Einigen T^4 -Zn-Al-, T^4 -Zn-Ga- und T^4 -Ga-Ge-Systemen", *Z. Metallkde.*, Vol 56, 1965, p 40-43.
- ⁸ G. Kresse and J. Furthmüller, "Efficient Iterative Schemes of Ab Initio Total-energy Calculations Using a Plane-wave Basis Set", *Phys. Rev. B*, Vol 54, 1996, p 11169-11186.
- ⁹ G. Kresse and J. Furthmüller, "Efficiency of Ab-initio Total Energy Calculations for Metals and Semi-conductors Using a Plane-wave Basis Set", *Computational Mater Sci.* Vol 6, 1996, p 15-50.
- ¹⁰ D. Vanderbilt, "Soft Self-consistent Pseudo Potential in a Generalized Eigenvalue Formalism", *Phys. Rev. B*, Vol 41, 1990, p 7892-7895.
- ¹¹ J.P. Perdew and Y. Wang, "Accurate and Simple Analytic Representation of the Electron-gas Correlation-energy", *Phys. Rev. B*, Vol 45, 1992, p 13244-13249.
- ¹² G. Ghosh and M. Asta, "First-principles Calculations of Structural Energetics of Al-TM(TM=Ti,Zr,Hf) Intermetallics", *Acta Mater.*, Vol 53, 2005, p 3225-3252.
- ¹³ A. van de Walle and G. Ceder, "Automating First-principles Phase Diagram Calculations", *J. Phase Equilibria*, Vol 23, 2002, p 348-359.
- ¹⁴ A. van de Walle, M. Asta and G. Ceder, "The Alloy Theoretic Automated Toolkit: A User Guide", *CALPHAD Journal*, Vol 26, 2002, p 539-553.
- ¹⁵ A. van de Walle and M. Asta, "Self-driven lattice-model Monte Carlo simulations of alloy thermodynamic properties and phase diagrams", *Modelling Simul. Mater. Eng.*, Vol 10, 2002, p 521-538.
- ¹⁶ P.D. Tepesch, G.D. Garbulsky and G. Ceder, "Model for Configurational Thermodynamics in Ionic Systems", *Phys. Rev. Lett.*, Vol 74, 1995, p 2272-2275.
- ¹⁷ G. Ceder, A. van der Ven, C. Marianetti, and D. Morgan, "First-principles Alloy Theory in Oxides", *Model. Simul. Mater. Sci. Eng.*, Vol 8, 2000, p 311-321.
- ¹⁸ J. M. Sanchez, F. Ducastelle and D. Gratias, "Generalized cluster description of multicomponent systems", *Physica*, Vol 128A, 1984, p 334-350.
- ¹⁹ P. Vinet, J.H. Rose, J. Ferrante, and J.R. Smith, "Universal Feature of the Equation of State in Solids", *J Phys:Condens Matter*, Vol 1, 1989, p 1941-1963.
- ²⁰ G.P. Vassilev, X.J. Liu, K. Ishida, "Reaction Kinetics and Phase Diagram Studies in the Ti-Zn System", *J. Alloys Comp.*, Vol 375, 2004, p 162-170.
- ²¹ G. Ghosh, S. Delsante, G. Borzone, M. Asta and R. Ferro, "Phase Stability and Cohesive Properties of Ti-Zn Intermetallics: First-principles Calculations and Experimental Results", submitted to *Acta Mater.*, 2005.
- ²² M.J. Mehl, B.M. Klein and A. Papaconstantopoulos, "First-Principles Calculations of Elastic Properties", in *Intermetallic Compounds: Principles*, J.H. Westbrook and R.L. Fleischer, Ed, Vol 1, John Wiley & Sons, NY, 1994, p 195-210.
- ²³ C.L. Fu, "Electronic, Elastic, and Fracture Properties of Trialuminides Alloys - Al_3Sc and Al_3Ti ", *J. Mater. Res.*, Vol 5, 1990, p 971-979.

- ²⁴ M.H. Yoo, C.L. Fu, "Fundamental-Aspects of Deformation and Fracture in High-Temperature Ordered Intermetallics", *ISIJ International*, Vol 31, 1991, p 1049-1062.
- ²⁵ M. Nakamura, K. Kimura, "Elastic-Constants of TiAl₃ and ZrAl₃ Single-Crystals", *J. Mater. Sci.*, Vol 26 ,1991, p 2208-2214.
- ²⁶ D.C. Wallace, *Thermodynamics of Crystals*, Wiley, New York, 1972.
- ²⁷ A.E. Carlsson and P.J. Meschter, "Ab Initio Calculations", in *Intermetallic Compounds: Principles*, J.H. Westbrook and R.L. Fleischer, Ed, Vol 1, John Wiley & Sons, NY, 1994, p 55-76.

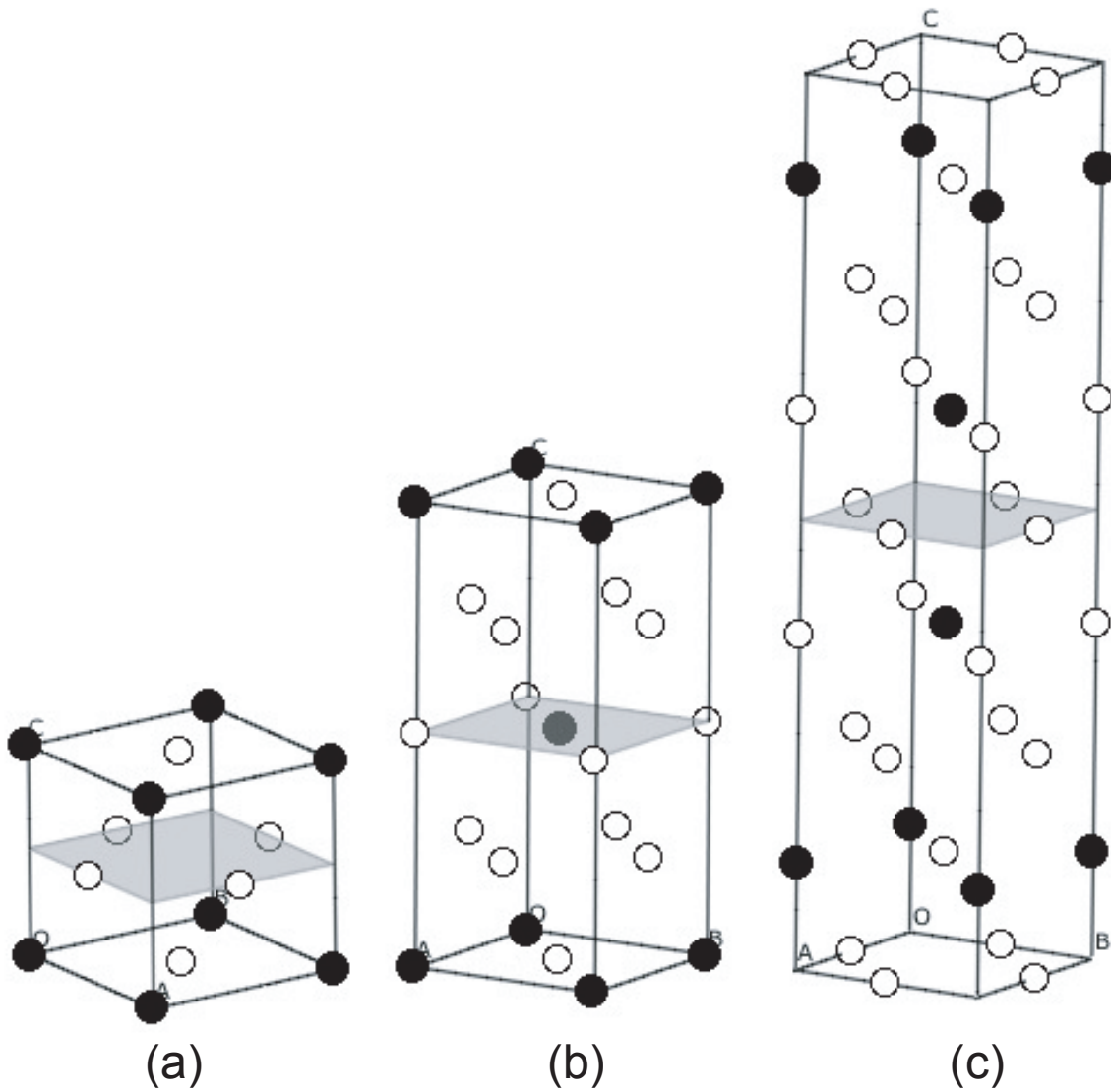


FIG. 1: Ball-and-stick model for the conventional unit cell of (a) $L1_2$, (b) DO_{22} , and (c) $DO_{23} \text{ Al}_3\text{Ti}$. Open and filled circles represent Al and Ti atoms, respectively. The Zn atoms are substituted in the Al sublattice only.

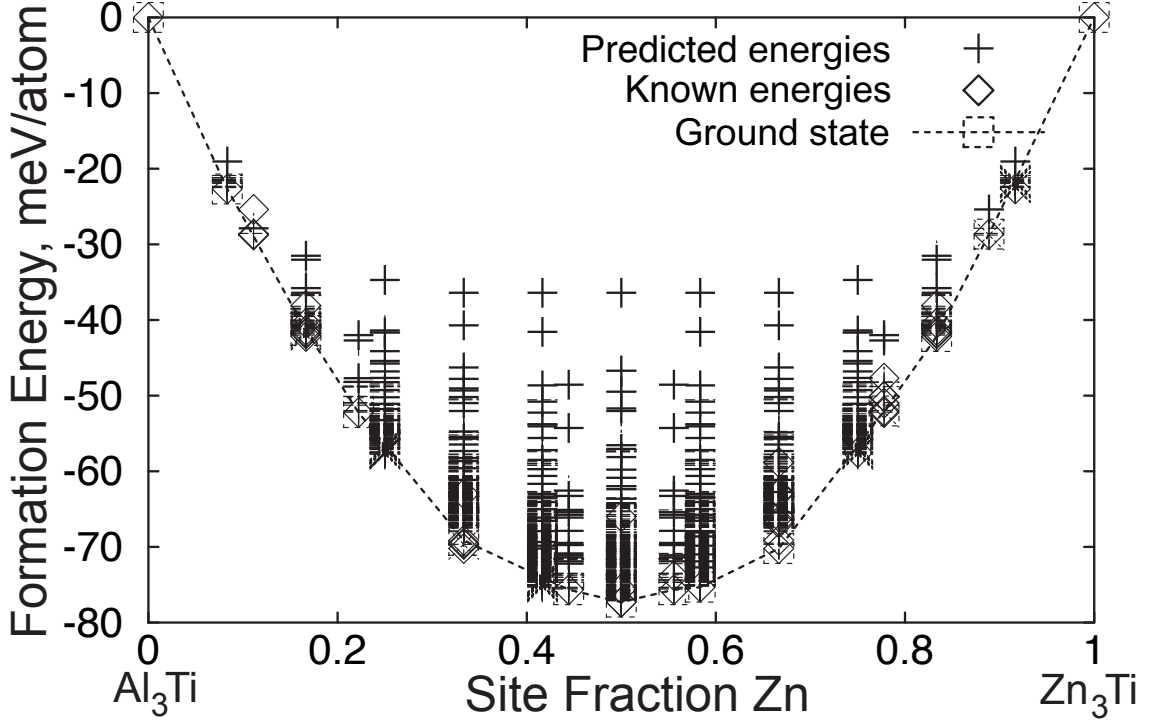


FIG. 2: Selected formation energies in the $L1_2$ - $(\text{Al},\text{Zn})_3\text{Ti}$ system. Diamonds denote the energies (predicted from the cluster expansion) for which the ab initio energy is known. The dotted line indicates the convex hull of these energies from which the ground states (squares) can be identified. The crosses denote predicted energies for a large database of generated structures (including all structures with at most 16 atoms per unit cell) that is used to verify that all ground states have been found. The reference states used to calculate the formation energies are $L1_2$ - Al_3Ti and $L1_2$ - Zn_3Ti .

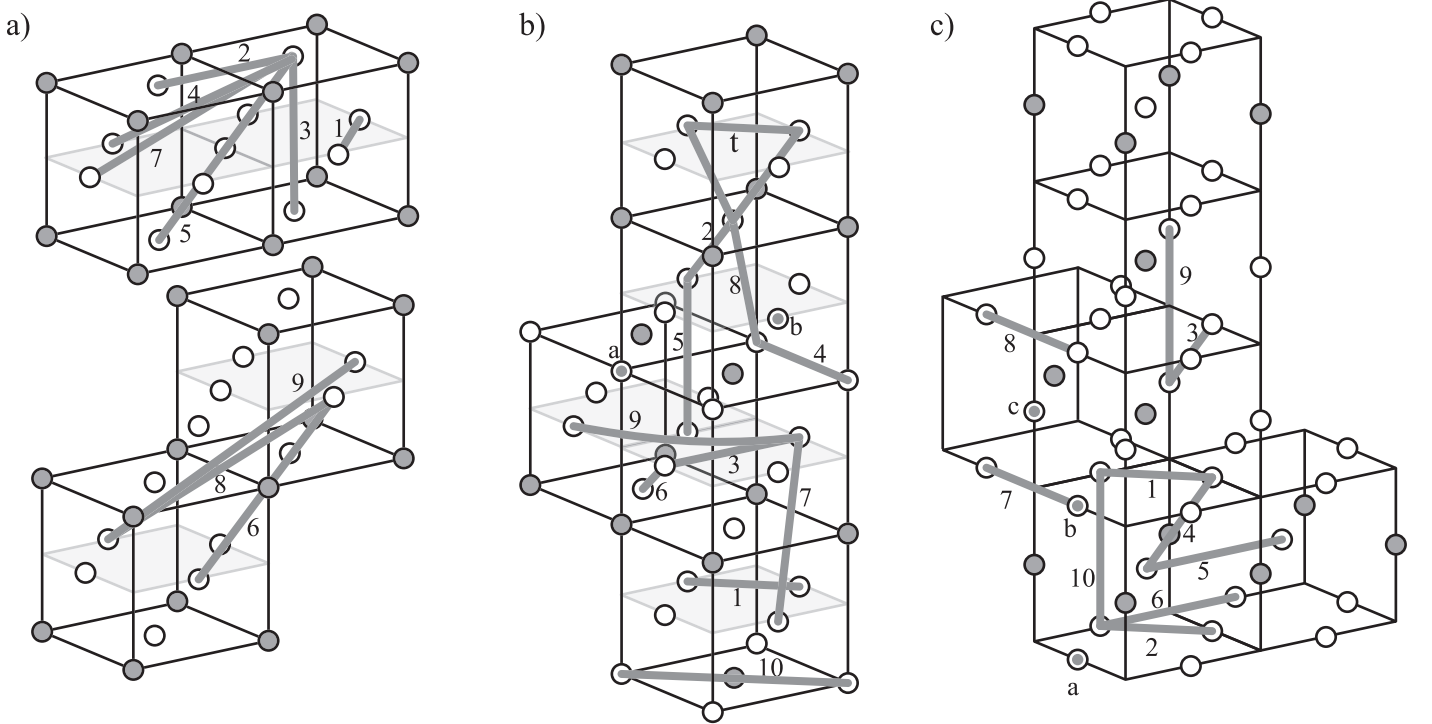


FIG. 3: Clusters included in the cluster expansions for the a) $L1_2$, b) DO_{22} and c) DO_{23} lattices. Point clusters are indicated by a,b,..., pair clusters by 1,2,... and the triplet by “t”. The clusters are enumerated in the same order as in the Table IV. For clarity, some of the clusters coordinates have been replaced by other, symmetrically equivalent, values.

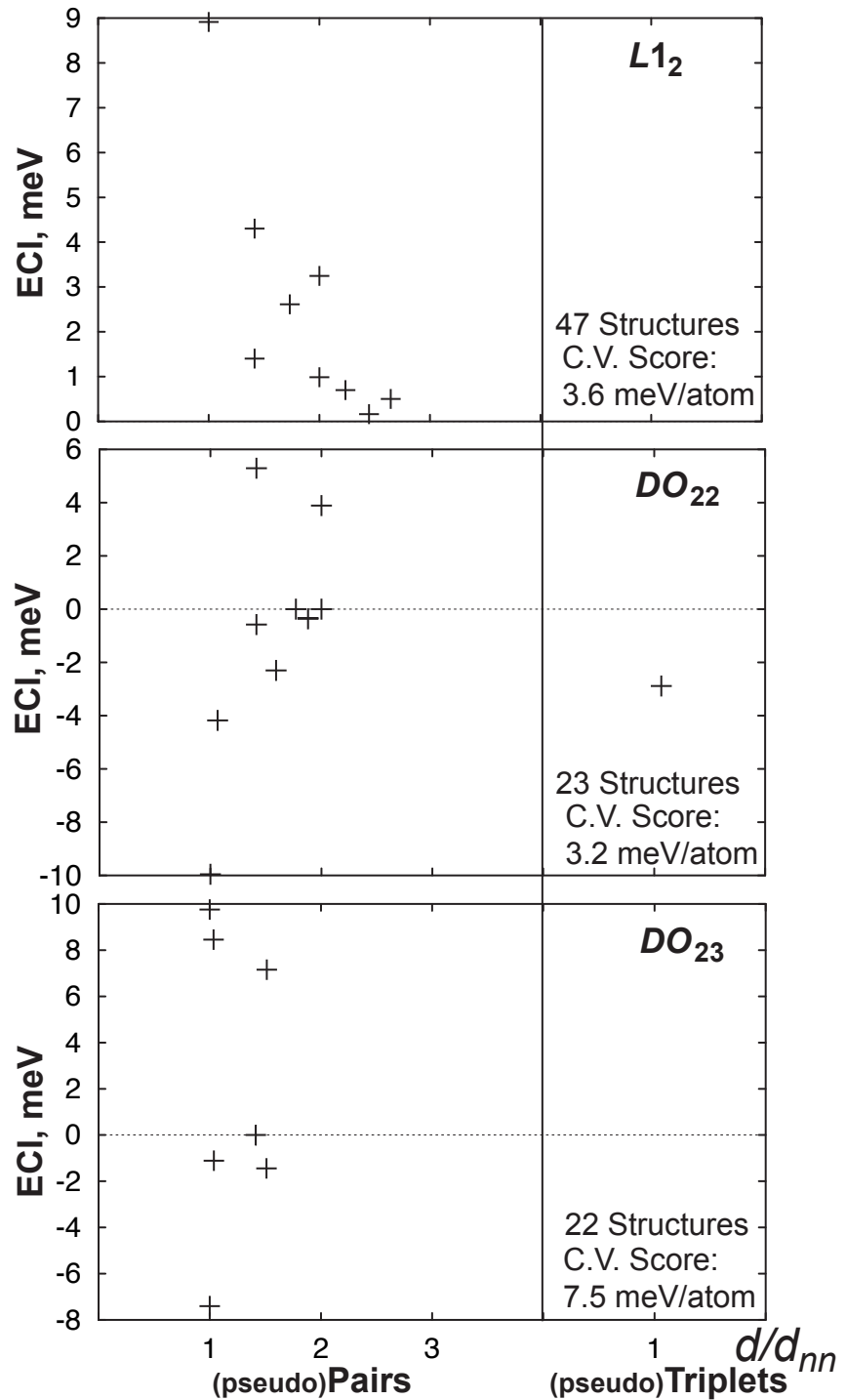


FIG. 4: Calculated ECIs versus cluster diameter (normalized by nearest neighbor distance) in $L1_2$ -, DO_{22} - and DO_{23} -(Al,Zn)₃Ti.

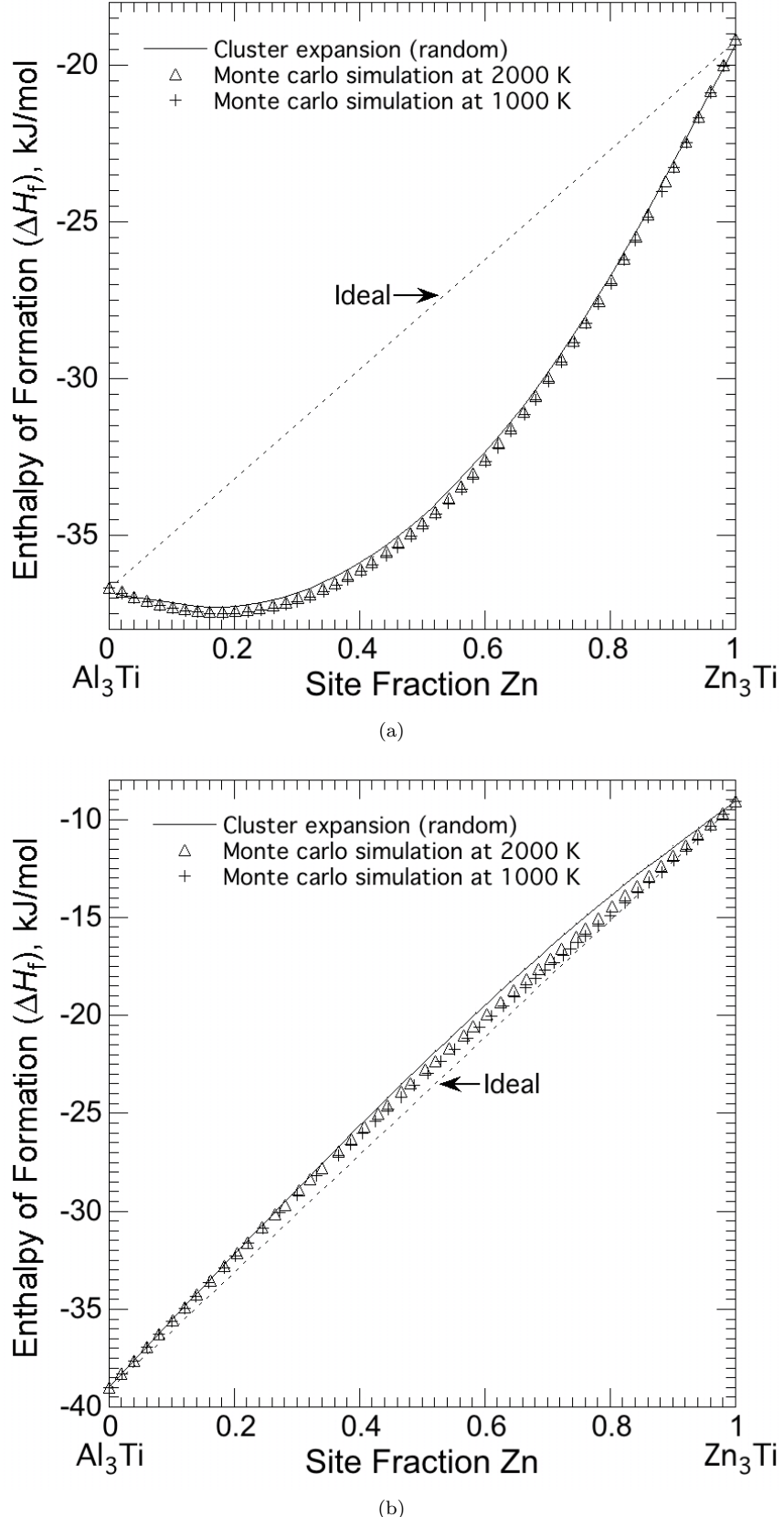


FIG. 5: Comparison of calculated heats of formation by cluster expansion and Monte Carlo simulation of (a) $L1_2$, and (b) DO_{22} phases along the pseudo-binary section Al_3Ti - Zn_3Ti . These demonstrate that the effect of short-range-order on the heat of formation is negligible as compared to that predicted by the cluster expansion for random mixing. The reference states are fcc-Al, hcp-Ti and hcp-Zn.

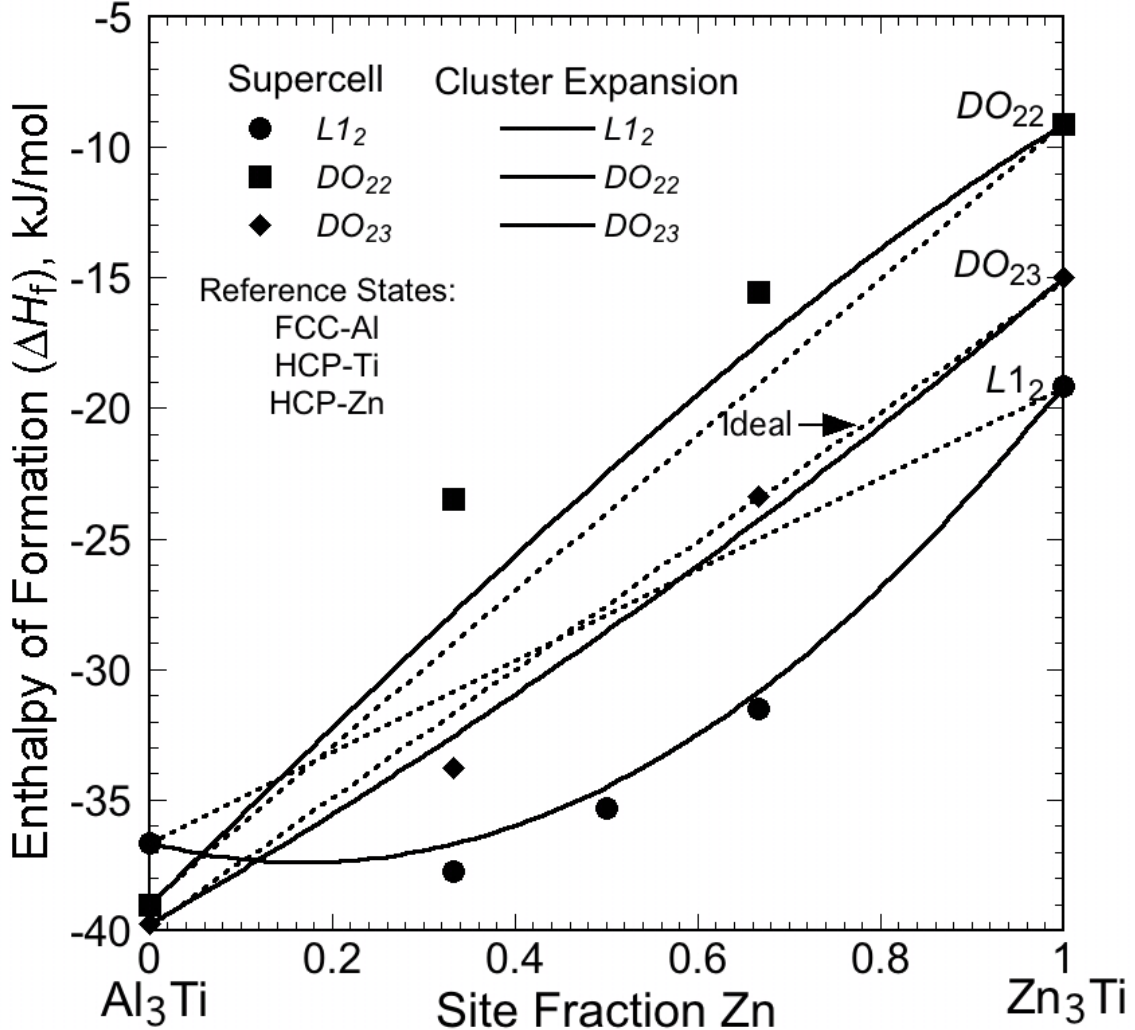


FIG. 6: Calculated heats of formation of $L1_2$, DO_{22} , and DO_{23} phases along the pseudo-binary section Al_3Ti-Zn_3Ti . The reference states are fcc-Al, hcp-Ti and hcp-Zn. The supercell results are shown to be in reasonably good with those predicted by the cluster expansion for random mixing.

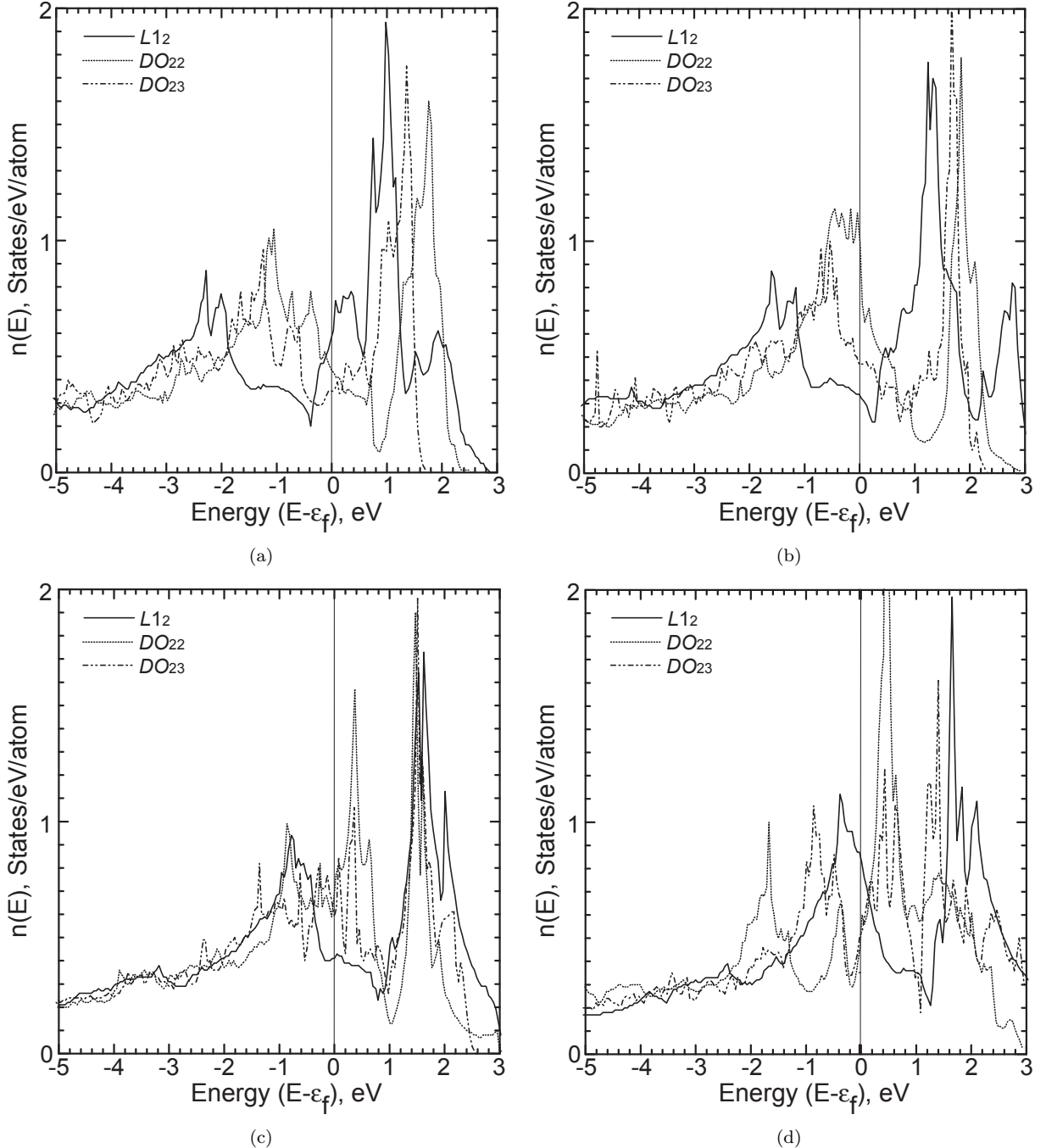


FIG. 7: A comparison of total density of states in $L1_2$, DO_{22} and DO_{23} along the pseudobinary section Al₃Ti-Zn₃Ti: (a) Al₃Ti and (b) (Al_{0.667}Zn_{0.333})₃Ti, (c) (Al_{0.333}Zn_{0.667})₃Ti and (d) Zn₃Ti.